

Astr 511: Galactic Astronomy

Winter Quarter 2015, University of Washington, Željko Ivezić

Lecture 8:

Stellar kinematics in the Milky Way

Parts I and II

Outline

1. Introduction

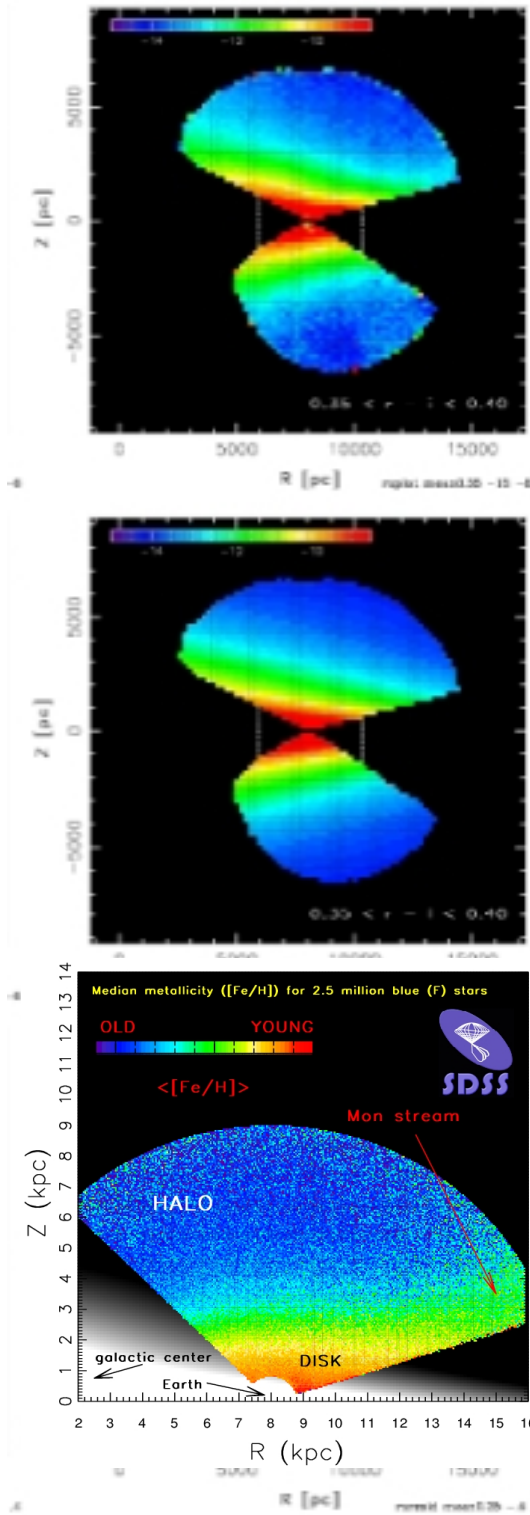
2. Stellar Kinematics: disk vs. halo

3. Stellar Kinematics: substructure

Reading:

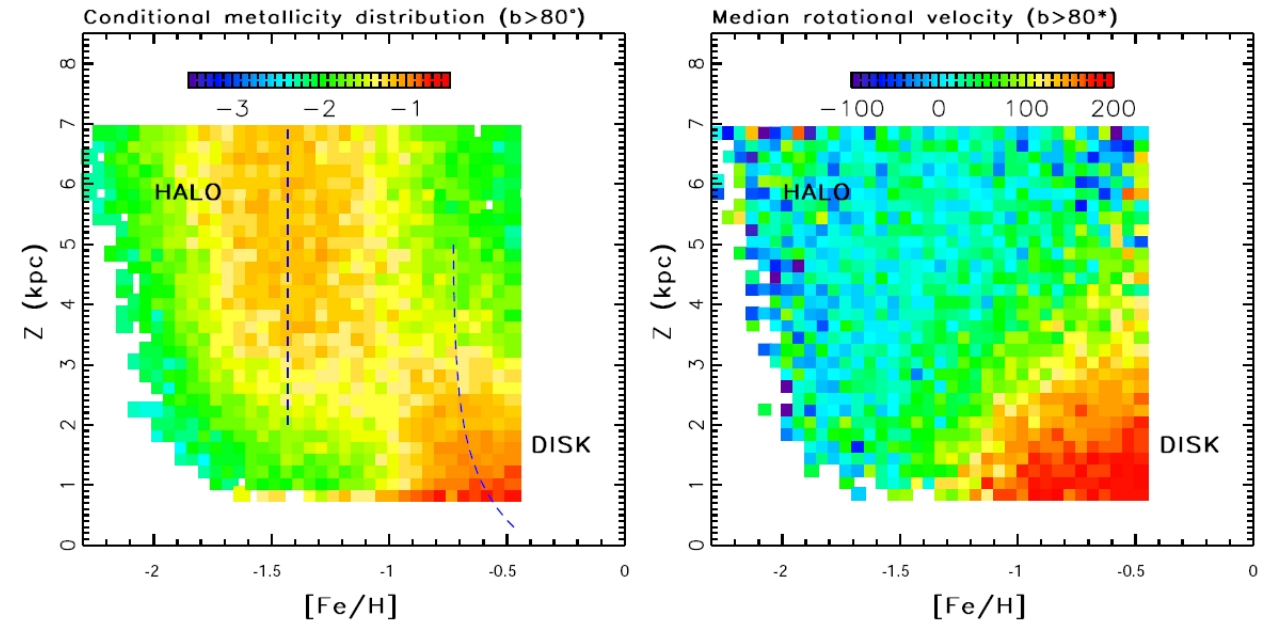
- Reid & Hawley: ch. 7 and 8; Binney & Merrifield: ch. 10
- Ivezić et al. 2008 (ApJ 684, 287): Sec. 3.4 and 4 at least
- Carollo et al. 2010 (ApJ 712, 692): Sec. 1 and 11 at least
- Bond et al. 2010 (ApJ 716, 1): Sec. 1 to 6 at least

$0.35 < r-i < 0.40$

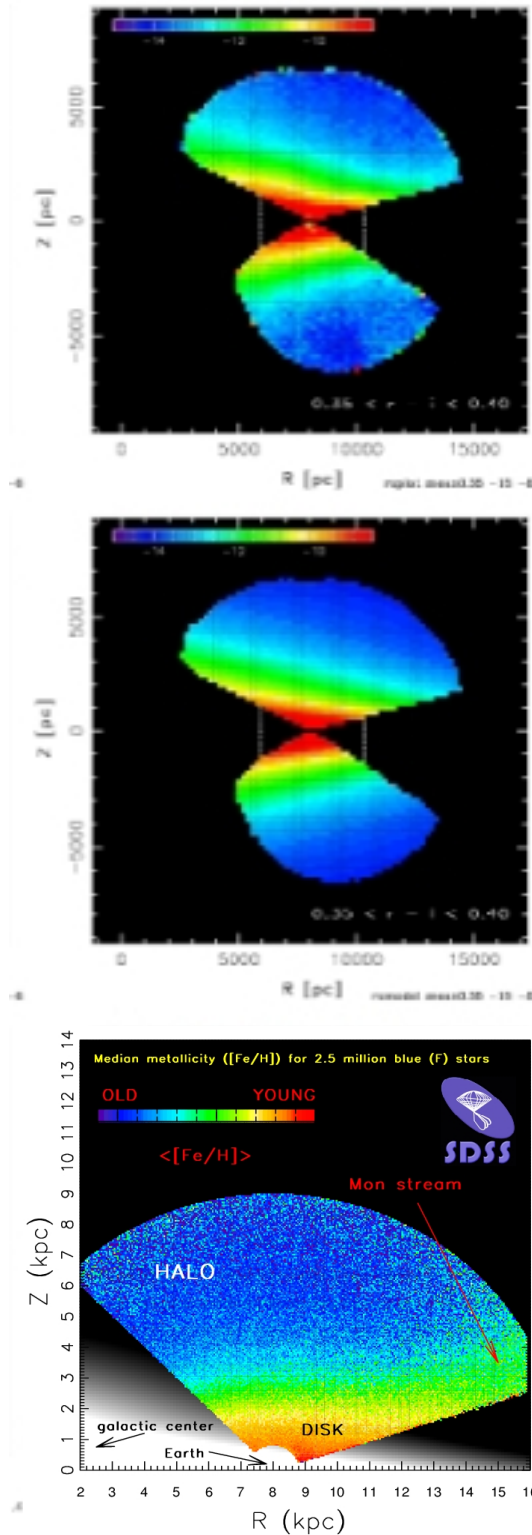


Dissecting the Milky Way with SDSS

- Panoramic view of the Milky Way, akin to observations of external galaxies; good support for standard Galactic models (with amazing signal-to-noise!)
- Metallicity mapping supports components inferred from number counts mapping
- Kinematics are correlated with metallicity
- Kinematics provide constraints on gravitational potential and initial conditions

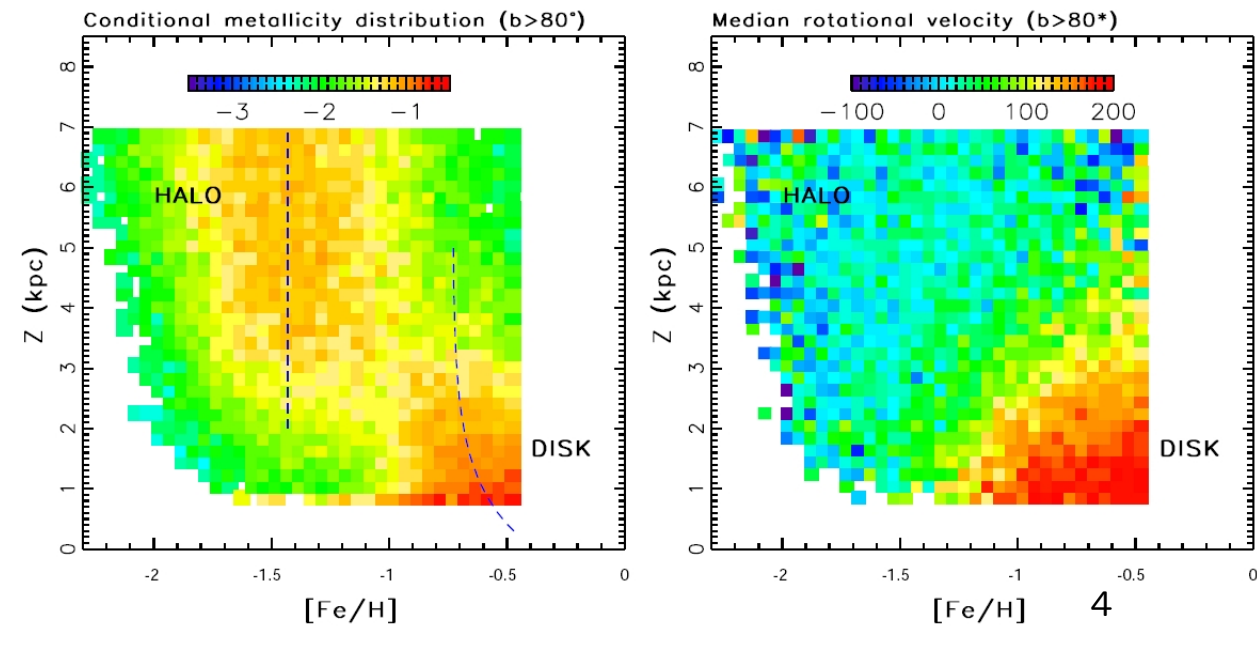


$0.35 < r-i < 0.40$



Dissecting the Milky Way with SDSS

- Kinematics present a much harder analysis problem than counts and $[Fe/H]$; instead of a single count value, or a scalar distribution function, at each position we need to study a 3-dimensional distribution function $p(v_\phi, v_R, v_Z)$!
- But first, how do we measure velocities?
- (we can't measure acceleration – except in special cases, such as orbits of stars in the Galactic center as we already discussed)



Velocity measurements

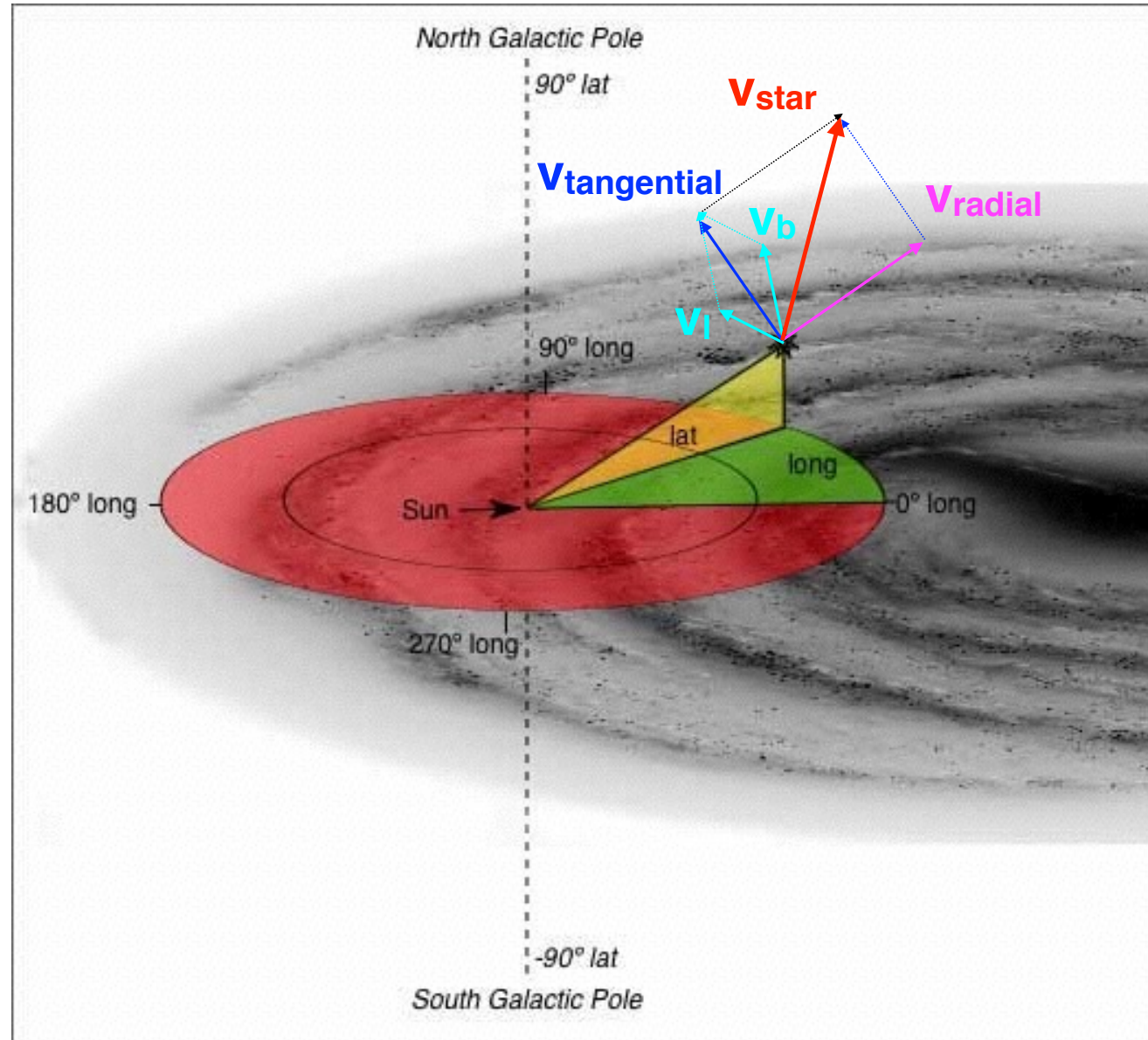
- Velocity can be expressed as a (vector) sum of the component along the line of sight, or radial velocity (v_{rad}), and the component perpendicular to the line of sight, or tangential velocity (v_{tan}).
- Radial velocity is measured from spectra; large modern stellar spectroscopic surveys, such as SDSS and RAVE, obtain errors of a few km/s (a revolution: close to 10^6 spectra!)
- Tangential velocity is measured from proper motion: angular displacement of stars on the sky (typically a tiny fraction of an arcsecond per year, but the record holder, Barnard's star, moves at 10 arcsec/yr); the two best large proper motion catalogs are based on the Hipparcos survey (an astrometric satellite, accuracy of \sim milliarcsec/yr for $V < 10$), and the SDSS-POSS catalog (5×10^7 stars, 3-5 mas/yr to $V < 20$)

Velocity measurements

- To get tangential velocity, v , from proper motion, μ , distance D must be known:

$$v = 4.74 \frac{\mu}{\text{mas/yr}} \frac{D}{\text{kpc}} \quad \text{km/s} \quad (1)$$

- At a distance of 1 kpc, and for proper motions good to \sim mas/yr, the tangential velocity errors are similar to radial velocity errors from SDSS and RAVE
- The advantage of radial velocity is that its measurement does not require distance, while the advantage of proper motion measurements is that they are much “cheaper”



Velocity measurements

- Assume that v_{rad} and the two components of tangential velocity, v_l (in the direction of the galactic longitude) and v_b (in the direction of the galactic latitude), are known.
- The Cartesian velocity components can be computed from

$$v_X^{obs} = -v_{rad} \cos(l) \cos(b) + v_b \cos(l) \sin(b) + v_l \sin(l)$$

$$v_Y^{obs} = -v_{rad} \sin(l) \cos(b) + v_b \sin(l) \sin(b) - v_l \cos(l)$$

$$v_Z^{obs} = -v_{rad} \sin(b) + v_b \cos(b)$$

- For completeness (right-handed coordinate system!):

$$X = R_\odot - D \cos(l) \cos(b)$$

$$Y = -D \sin(l) \cos(b)$$

$$Z = D \sin(b)$$

Velocity measurements

- Assume that v_{rad} and the two components of tangential velocity, v_l (in the direction of the galactic longitude) and v_b (in the direction of the galactic latitude), are known.
- The Cartesian velocity components can be computed from

$$v_X^{obs} = -v_{rad} \cos(l) \cos(b) + v_b \cos(l) \sin(b) + v_l \sin(l)$$

$$v_Y^{obs} = -v_{rad} \sin(l) \cos(b) + v_b \sin(l) \sin(b) - v_l \cos(l)$$

$$v_Z^{obs} = -v_{rad} \sin(b) + v_b \cos(b)$$

- Locally, these components are related to more traditional nomenclature as $v_X = -U$, $v_Y = -V$, and $v_Z = W$.

Velocity measurements

- How do we go from the measured v_X , v_Y , and v_Z for a star, to **its own galactocentric** v_R , v_ϕ , and v_Z ?
- First, **we need to account for our motion**. When reporting radial velocity, the projection of Earth's orbital motion (up to 30 km/s!) is typically corrected. Hence, we *only* need to correct for the solar motion around the center of the Milky Way (v^\odot):

$$\begin{aligned}v_X^{obs} &= v_X^* + v_X^\odot \\v_Y^{obs} &= v_Y^* + v_Y^\odot \\v_Z^{obs} &= v_Z^* + v_Z^\odot\end{aligned}$$

where v^* corresponds to a **star's own motion** around the center of the Milky Way (this is what we want to get)

Velocity measurements

- The solar motion is traditionally decomposed into the **rotational** motion of the Local Standard of Rest and the solar **peculiar** motion:

$$\begin{aligned}v_X^\odot &= v_X^{\odot, pec} \\v_Y^\odot &= -v_{LSR} + v_Y^{\odot, pec} \\v_Z^\odot &= v_Z^{\odot, pec}\end{aligned}$$

- **Note the minus sign in front of v_{LSR} !** Usually it is assumed that $v_{LSR} = 220 \text{ km/s}$ (based on HI measurements by Gunn, Knapp & Tremaine 1979), but some recent papers claim that it could be off by as much as 20-30 km/s (some methods are sensitive to uncertain $R_* = 8.0 \text{ kpc!}$)

Velocity measurements

- The solar peculiar motion is obtained by averaging the motions of a large number of stars from the (local) solar neighbourhood (so that their peculiar velocities cancel out)
- Currently the best measurement of the solar peculiar motion is based on Hipparcos data (Dehnen & Binney 1998):
 $v_X^{\odot,pec} = -10.0 \text{ km/s}$, $v_Y^{\odot,pec} = -5.3 \text{ km/s}$, $v_Z^{\odot,pec} = 7.2 \text{ km/s}$.
- But recently they revisited this problem (Schönrich, Binney & Dehnen 2010):
 $v_X^{\odot,pec} = -11.1 \text{ km/s}$, $v_Y^{\odot,pec} = -12.2 \text{ km/s}$, $v_Z^{\odot,pec} = 7.3 \text{ km/s}$
- The measured mean Y velocity component depends greatly on the selected type of stars (the so-called *asymmetric drift*, more about that later).

Velocity measurements

- How do we go from the measured v_X , v_Y , and v_Z for a star, to **its own galactocentric** v_R , v_ϕ , and v_Z ?
- First, we need to account for our motion:

$$\begin{aligned}v_X^* &= v_X^{obs} - v_X^\odot \\v_Y^* &= v_Y^{obs} - v_Y^\odot \\v_Z^* &= v_Z^{obs} - v_Z^\odot\end{aligned}$$

- After (v_X^*, v_Y^*, v_Z^*) are known, and assuming that the position of the star, (X^*, Y^*, Z^*) , is known too, this is simply a coordinate system transformation ($R = \sqrt{X^2 + Y^2}$)

$$\begin{aligned}v_R^* &= v_X^* \frac{X^*}{R^*} + v_Y^* \frac{Y^*}{R^*} \\v_\phi^* &= -v_X^* \frac{Y^*}{R^*} + v_Y^* \frac{X^*}{R^*}\end{aligned}$$

Velocity Distribution Function

- Given (v_R^*, v_ϕ^*, v_Z^*) measurements, how do we analyze them? (hereafter, droping superscript *)
- For a given control volume, dV , positioned at (X, Y, Z) , and using an appropriately chosen subsample of stars described by *tags* (e.g. $[Fe/H]$, M_r , mass, age), we can define a multi-dimensional distribution function, $p(v_R, v_\phi, v_Z, X, Y, Z, \text{tags})$, such that the number of stars, dN , in that (spatial) volume with velocities in the range v_i to $v_i + dv_i$, with $i = R, \phi, Z$, is

$$dN(X, Y, Z, v_R, v_\phi, v_Z, \text{tags}) = \\ p(v_R, v_\phi, v_Z, X, Y, Z, \text{tags}) dV dv_R dv_\phi dv_Z$$

Velocity Distribution Function

- The normalization of this (complex!) function depends on the **spatial variation of density profiles** which we already studied, metallicity distribution, and the **luminosity function** for each Galaxy component (e.g. disk and halo, which in principle also depend on position). Assuming only three tags (M_r , $[Fe/H]$, age), we can formally write ($|$ means “given”)

$$\begin{aligned} p(v_R, v_\phi, v_Z, X, Y, Z, M_r, [Fe/H], \text{age}) = \\ \times f(v_R, v_\phi, v_Z | X, Y, Z, M_r, [Fe/H], \text{age}) \\ \times \rho(X, Y, Z | M_r, [Fe/H], \text{age}) \\ \times \Phi(M_r | [Fe/H], \text{age}) \times p([Fe/H] | \text{age}) \times p(\text{age}) \end{aligned}$$

- Here, we would like to measure and understand theoretically the **shape** of $f(v_R, v_\phi, v_Z | X, Y, Z, \text{tags})$ (leaving normalization aside for now), and how it varies with (X, Y, Z) and as a function of various *tags*.

Velocity Distribution Function

- Traditionally, the measurements were confined to the solar neighborhood (e.g. practically all Hipparcos stars are closer than 100 pc); hence, we knew little about the spatial variation of $f(v_R, v_\phi, v_Z | X, Y, Z, \text{tags})$. Also, there are very few halo stars (< 1%) in local samples, so the variation as a function of metallicity was not well measured either.
- Local measurements of smallish samples were consistent with a 3-dimensional gaussian distribution: **the Schwarzschild velocity ellipsoid**

$$f(v_R, v_\phi, v_Z) = \prod_{i=1}^3 G(\bar{v}_i, \sigma_i)$$

where \bar{v}_i are *mean velocities*, and σ_i are *velocity dispersions* in the principal directions. In a special case when the velocity ellipsoid is aligned with the coordinate system, the principal directions are the coordinate axes.

Velocity Distribution Function

Within the paradigm of **velocity ellipsoid**, some questions to ask are:

1. Is this gaussian approximation supported by the data? E.g. are there localized cold streams? Multiple gaussian components (disk vs. halo, thin vs. thick disk)?
2. What are the values of \bar{v}_i and σ_i , and do they depend on position and tags such as metallicity and age?
3. What is the orientation of the velocity ellipsoid?
4. Can we interpret velocity ellipsoid with some “reasonable” gravitational potentials?

Before discussing recent progress enabled by SDSS data (e.g., Bond et al. 2010, ApJ 716, 1), we will review derivation of the Jeans Equations (more details are in “Review Lecture: Stellar kinematics: a bit of theory”).

Stellar Dynamics and the Boltzmann Equation

The positions and motions of stars can be described by a phase-space distribution function $f(\mathbf{x}, \mathbf{v}, t)$ (aka the phase-space probability density)

The time evolution of $f(\mathbf{x}, \mathbf{v}, t)$ is described by Newtonian dynamics

Assuming that stars can be neither created nor destroyed, a **continuity equation** can be applied to $f(\mathbf{x}, \mathbf{v}, t)$. In six-dimensional space described by $w_i = (\mathbf{x}, \mathbf{v}) = (x_1, x_2, x_3, v_1, v_2, v_3)$,

$$\frac{\partial f(\mathbf{w}, t)}{\partial t} + \sum_{i=1}^6 \frac{\partial (f(\mathbf{w}, t) \dot{w}_i)}{\partial w_i} = 0. \quad (2)$$

The collisionless Boltzmann Equation

$$\frac{\partial(f\dot{w}_i)}{\partial w_i} = \dot{w}_i \frac{\partial f}{\partial w_i} + f \frac{\partial \dot{w}_i}{\partial w_i} \quad (3)$$

Note that the last term is either $(\partial v_i / \partial x_i)$, or $(\partial \dot{v}_i / \partial v_i)$.

This term is always 0: in the first case because v_i and x_i are independent coordinates, and in the second case because $\dot{v}_i = -(\partial \Phi / \partial x_i)$, and Φ does not depend on velocity (because it's gravitational potential). Hence,

$$\frac{\partial f(\mathbf{w}, t)}{\partial t} + \sum_{i=1}^6 \dot{w}_i \frac{\partial f(\mathbf{w}, t)}{\partial w_i} = 0. \quad (4)$$

The collisionless Boltzmann Equation (CBE)

$$\frac{\partial f(\mathbf{w}, t)}{\partial t} + \sum_{i=1}^6 \dot{w}_i \frac{\partial f(\mathbf{w}, t)}{\partial w_i} = 0. \quad (5)$$

In other forms:

$$\frac{\partial f}{\partial t} + \sum_{i=1}^3 \left[v_i \frac{\partial f}{\partial x_i} - \frac{\partial \Phi}{\partial x_i} \frac{\partial f}{\partial v_i} \right] = 0 \quad (6)$$

$$\frac{\partial f}{\partial t} + \mathbf{v} \nabla f = \nabla \Phi \frac{\partial f}{\partial \mathbf{v}} \quad (7)$$

The collisionless Boltzmann Equation (CBE)

The last (vector) notation is the most useful one for expressing the collisionless Boltzmann equation in arbitrary coordinate systems

Very difficult to solve (and hence not terribly useful from that standpoint), but forms the basis for deriving [the Jeans equations](#).

A side note: encounters between stars require another term.

Another side note: the radiative transfer equation is also a special case of the general Boltzmann Equation (in the limit that all particles move at the same speed).

The Moment Equations

Now let us integrate the CBE expressed in form (4) over all velocities:

$$\int \frac{\partial f}{\partial t} d^3v + \int v_i \frac{\partial f}{\partial x_i} d^3v - \frac{\partial \Phi}{\partial x_i} \int \frac{\partial f}{\partial v_i} d^3v = 0. \quad (8)$$

How do we evaluate these integrals? Two rules:

1. Derivative wrt x , or a function of x , can be taken out
2. Introduce notation

$$\int g(v) f d^3v = \langle g \rangle \int f d^3v \quad (9)$$

where

$$\nu(x) = \int f d^3v \quad (10)$$

is the number density as a function of position.

The Moment Equations

Then

$$\int \frac{\partial f}{\partial t} d^3v + \int v_i \frac{\partial f}{\partial x_i} d^3v - \frac{\partial \Phi}{\partial x_i} \int \frac{\partial f}{\partial v_i} d^3v = 0. \quad (11)$$

with

$$\bar{v}_i \equiv \frac{1}{\nu} \int f v_i d^3v, \quad (12)$$

becomes

$$\frac{\partial \nu}{\partial t} + \frac{\partial(\nu \bar{v}_i)}{\partial x_i} = 0. \quad (13)$$

This is just the continuity equation for the stellar number density in real space.

More interesting results are obtained by multiplying the CBE with higher powers of \mathbf{v} .

The Moment Equations

E.g. take the first velocity moment of the CBE. Then

$$\int \frac{\partial f}{\partial t} d^3 v + \int v_i \frac{\partial f}{\partial x_i} d^3 v - \frac{\partial \Phi}{\partial x_i} \int \frac{\partial f}{\partial v_i} d^3 v = 0. \quad (14)$$

becomes

$$\frac{\partial}{\partial t} \int f v_j d^3 v + \int v_i v_j \frac{\partial f}{\partial x_i} d^3 v - \frac{\partial \Phi}{\partial x_i} \int v_j \frac{\partial f}{\partial v_i} d^3 v = 0. \quad (15)$$

We can use the divergence theorem to manipulate the last term

$$\int v_j \frac{\partial f}{\partial v_i} d^3 v = - \int \frac{\partial v_j}{\partial v_i} f d^3 v = - \int \delta_{ij} f d^3 v = -\delta_{ij} \nu, \quad (16)$$

Note that

$$v_j \frac{\partial f}{\partial v_i} = -f \frac{\partial v_j}{\partial v_i} + \frac{\partial(v_j f)}{\partial v_i} \quad (17)$$

and the last term must be 0 when the integration surface is expended to infinity (where f must vanish).

The Moment Equations

Eq.(16) can be substituted into (15) giving

$$\frac{\partial(\nu\bar{v}_j)}{\partial t} + \frac{\partial(\nu\bar{v}_i\bar{v}_j)}{\partial x_i} + \nu \frac{\partial\Phi}{\partial x_j} = 0, \quad (18)$$

where

$$\bar{v}_i\bar{v}_j \equiv \frac{1}{\nu} \int v_i v_j f d^3 v. \quad (19)$$

This is an equation of momentum conservation.

Each velocity can be expressed as a sum of the mean value (aka streaming motion) and the so-called peculiar velocity

$$v_i = \bar{v}_i + w_i \quad (20)$$

where $\bar{w}_i = 0$ by definition.

The Moment Equations

Then

$$\sigma_{ij}^2 \equiv \overline{w_i w_j} = \overline{(v_i - \bar{v}_i)(v_j - \bar{v}_j)} = \overline{v_i v_j} - \bar{v}_i \bar{v}_j. \quad (21)$$

At each point x the symmetric tensor σ^2 defines an ellipsoid whose principal axes run parallel to σ^2 's eigenvectors and whose semi-axes are proportional to the square roots of σ^2 's eigenvalues. This is called the **velocity ellipsoid** at x .

The Jeans Equations

The continuity equation:

$$\frac{\partial \nu}{\partial t} + \frac{\partial(\nu \bar{v}_i)}{\partial x_i} = 0. \quad (22)$$

and the momentum equation

$$\nu \frac{\partial \bar{v}_j}{\partial t} + \nu \bar{v}_i \frac{\partial \bar{v}_j}{\partial x_i} = -\nu \frac{\partial \Phi}{\partial x_j} - \frac{\partial(\nu \sigma_{ij}^2)}{\partial x_i} \quad (23)$$

The term $-\nu \sigma_{ij}^2$ is a **stress tensor** – it describes an anisotropic pressure.

Note that **the system is not closed**: there is no “equation of state”! The multiplication by higher powers of ν doesn’t help – need an *ansatz*. In practice one assumes a particular form for σ_{ij}^2 , e.g. for isotropic velocity dispersion $\sigma_{ij}^2 = \sigma^2 \delta_{ij}$

The Jeans Equations

Specialization for an axially symmetric system:

First express the CBE in cylindrical coordinates

$$\frac{\partial f}{\partial t} + \dot{R}\frac{\partial f}{\partial R} + \dot{\phi}\frac{\partial f}{\partial \phi} + \dot{z}\frac{\partial f}{\partial z} + \dot{v}_R\frac{\partial f}{\partial v_R} + \dot{v}_\phi\frac{\partial f}{\partial v_\phi} + \dot{v}_z\frac{\partial f}{\partial v_z} = 0 \quad (24)$$

With $\dot{R} \equiv v_R$, $\dot{\phi} \equiv v_\phi/R$, and $\dot{z} \equiv v_z$, and

$$\dot{v}_R = -\frac{\partial \Phi}{\partial R} + \frac{v_\phi^2}{R} \quad (25)$$

$$\dot{v}_\phi = -\frac{1}{R}\frac{\partial \Phi}{\partial \phi} - \frac{v_R v_\phi}{R} \quad (26)$$

$$\dot{v}_z = -\frac{\partial \Phi}{\partial z} \quad (27)$$

we get

The Jeans Equations

$$\frac{\partial f}{\partial t} + v_R \frac{\partial f}{\partial R} + v_z \frac{\partial f}{\partial z} + \left[\frac{v_\phi^2}{R} - \frac{\partial \Phi}{\partial R} \right] \frac{\partial f}{\partial v_R} - \frac{v_R v_\phi}{R} \frac{\partial f}{\partial v_\phi} - \frac{\partial \Phi}{\partial z} \frac{\partial f}{\partial v_z} = 0 \quad (28)$$

where it was assumed that $\partial/\partial\phi \equiv 0$.

Now we multiply by v_R , v_z and v_ϕ , and integrate over all velocities to get (assuming steady state)

$$\begin{aligned} \frac{\partial(\nu \bar{v}_R^2)}{\partial R} + \frac{\partial \nu \bar{v}_R \bar{v}_z}{\partial z} + \nu \left(\frac{\bar{v}_R^2 - \bar{v}_\phi^2}{R} + \frac{\partial \Phi}{\partial R} \right) &= 0, \\ \frac{\partial(\nu \bar{v}_R \bar{v}_\phi)}{\partial R} + \frac{\partial(\nu \bar{v}_\phi \bar{v}_z)}{\partial z} + \frac{2\nu}{R} \bar{v}_\phi \bar{v}_R &= 0, \\ \frac{\partial(\nu \bar{v}_R \bar{v}_z)}{\partial R} + \frac{\partial(\nu \bar{v}_z^2)}{\partial z} + \frac{\nu \bar{v}_R \bar{v}_z}{R} + \nu \frac{\partial \Phi}{\partial z} &= 0. \end{aligned} \quad (29)$$

This set of equations is very powerful for interpreting motions of stars in the Galaxy.

SDSS-POSS proper motion measurements

- The Munn et al. (2004 AJ, 127, 3034) catalog
 - recalibrated POSS astrometry using galaxies
 - 100,000 quasars (360 per Schmidt plate) for quality assessment: random errors 3 mas/yr (per coordinate) to $r < 18$, increases to 6 mas/yr at $r = 20$, systematic errors ~ 0.3 mas/yr
 - publicly available as part of SDSS Data Release 6
 - Over 30,000,000, mostly main sequence, stars: the largest accurate proper motion catalog (until Gaia and LSST)

Independent Test of Systematic Errors

- There are lots of quasars in SDSS-POSS sample, and quasars don't move as fast as \sim mas/yr.

4

BOND ET AL.

Vol. 716

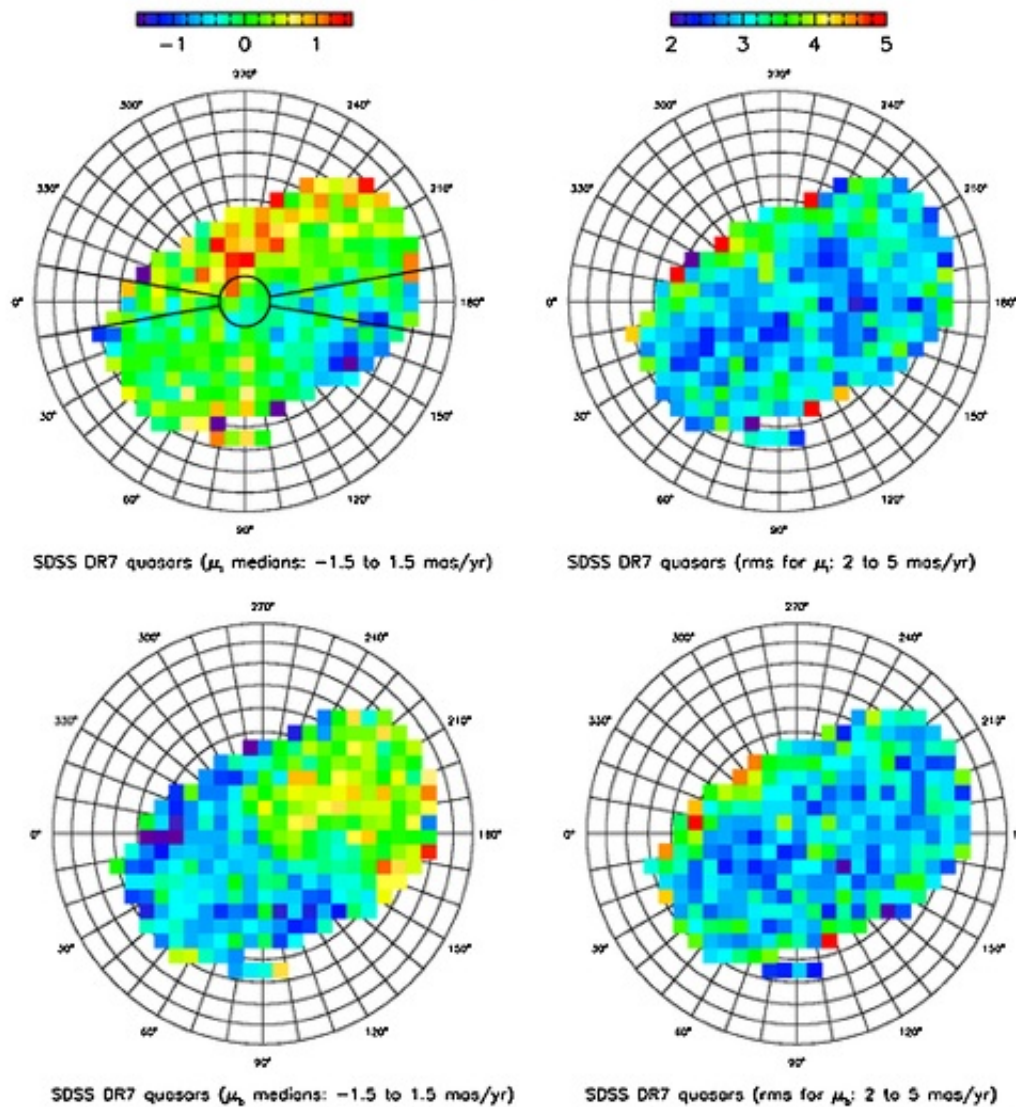


Figure 1. Behavior of proper-motion measurements for 60,000 spectroscopically confirmed SDSS quasars with $b > 0^\circ$. The color-coded maps (see the legend on top, units are mas yr^{-1}) show the distribution of the median (left) and rms (right) for the longitudinal (top) and latitudinal (bottom) proper-motion components in a Lambert projection of the northern Galactic cap. The median number of quasars per pixel is ~ 250 . For both components, the scatter across the sky is 0.60 mas yr^{-1} . The median proper motion for the full quasar sample is 0.15 mas yr^{-1} in the longitudinal direction, and $-0.20 \text{ mas yr}^{-1}$ in the latitudinal direction. The thick line in the top-left panel shows the selection boundary for the "meridional plane" sample.

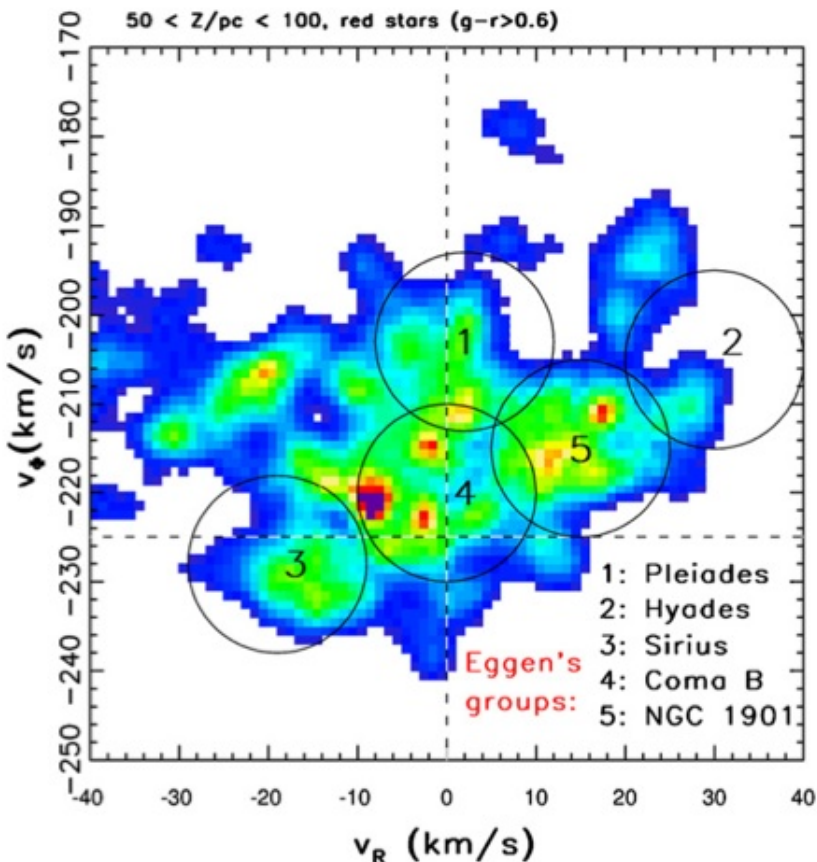
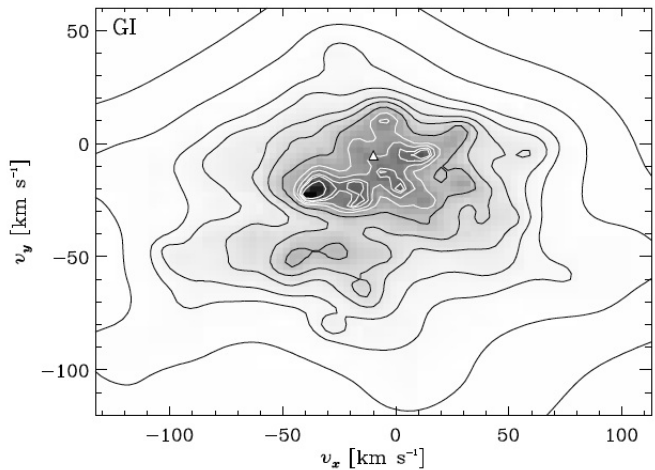


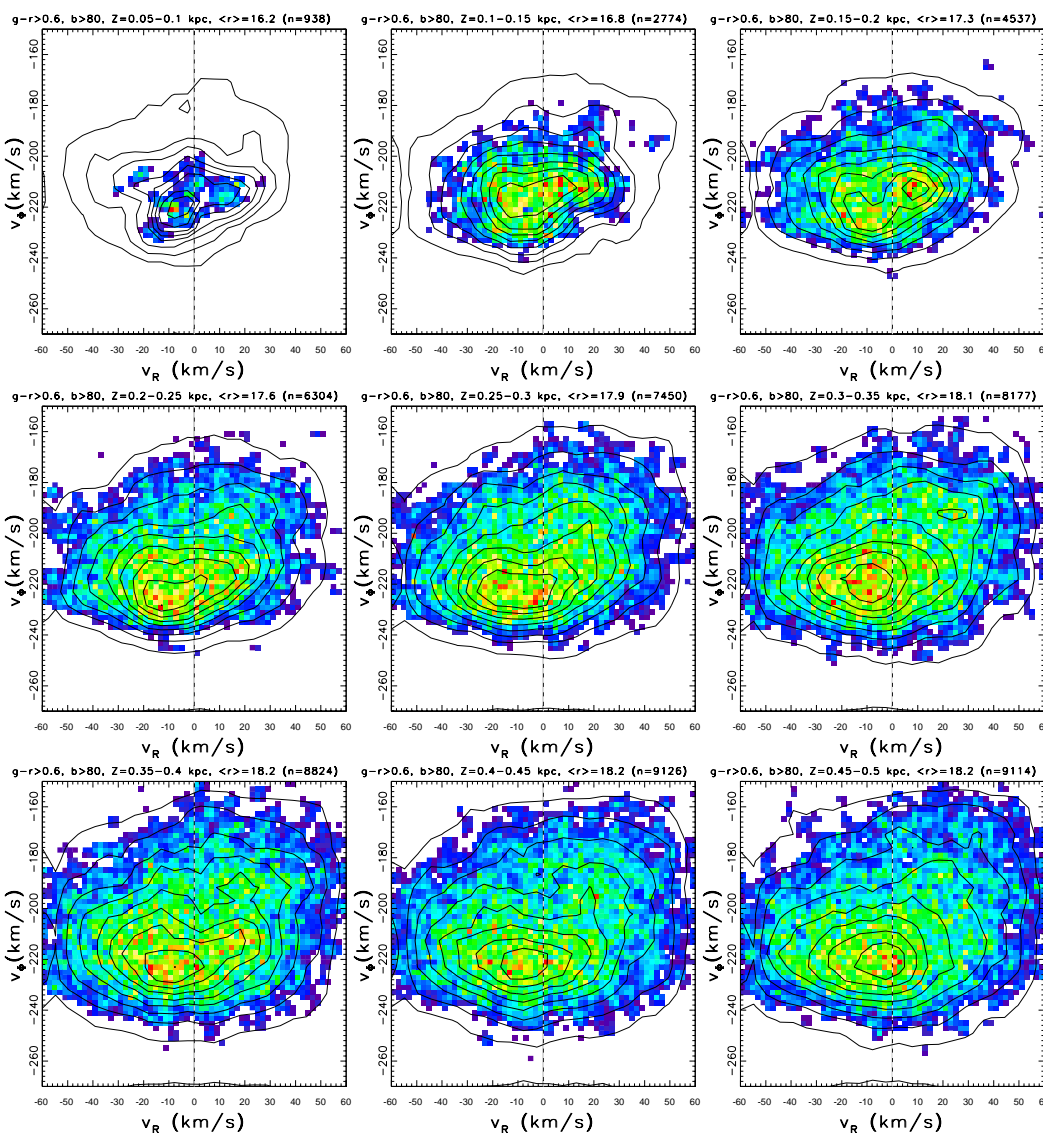
Figure 4. Similar to the top-left panel in Figure 3, except that stars are selected from a distance bin that corresponds to *HIPPARCOS* sample ($Z = 50\text{--}100$ pc). The positions of Eggen's moving groups (Eggen 1996) are marked by circles, according to the legend in the bottom-right corner. The horizontal line at $v_\phi = -225 \text{ km s}^{-1}$ corresponds to vanishing heliocentric motion in the rotational direction.



Kinematics for nearby stars

- A good summary/definitive analysis of the local Hipparcos sample: Dehnen & Binney (1998, MNRAS 298, 387).
- Within about 100 pc from the plane, the kinematics show a lot of structure: **multiple peaks** (first advocated by Eggen, later demonstrated in Hipparcos data by Dehnen, see bottom left)

Kinematics for nearby stars



- Within about 100 pc from the plane, the kinematics show a lot of structure: **multiple peaks** (first advocated by Eggen, later demonstrated in Hipparcos data by Dehnen)
- Panels:** $f(v_R, v_\phi)$ for red (K and M) main-sequence stars towards the north galactic pole; determined using SDSS-POSS proper motions, in nine 50pc thick Z slices, from 50 pc to 500 pc
- Beyond 100 pc from the plane, the velocity distribution becomes more similar to a gaussian; however, deviations are clearly detected (due to a large number of stars and well-controlled errors)

Oort's constants:

$$A \equiv \frac{1}{2} \left(\frac{v_c}{R} - \frac{dv_c}{dR} \right)_{R_\odot} = -\frac{1}{2} \left(R \frac{d\Omega}{dR} \right)_{R_\odot} \quad (30)$$

$$B \equiv -\frac{1}{2} \left(\frac{v_c}{R} + \frac{dv_c}{dR} \right)_{R_\odot} = -\left(\frac{1}{2} R \frac{d\Omega}{dR} + \Omega \right)_{R_\odot} = A - \Omega_\odot \quad (31)$$

Then

$$\kappa_\odot^2 = -4B(A - B) = -4B\Omega_\odot \quad (32)$$

In the solar neighborhood,

$$A = 14.5 \pm 1.5 \text{ km/s/kpc}, \quad B = -12 \pm 3 \text{ km/s/kpc}, \quad (33)$$

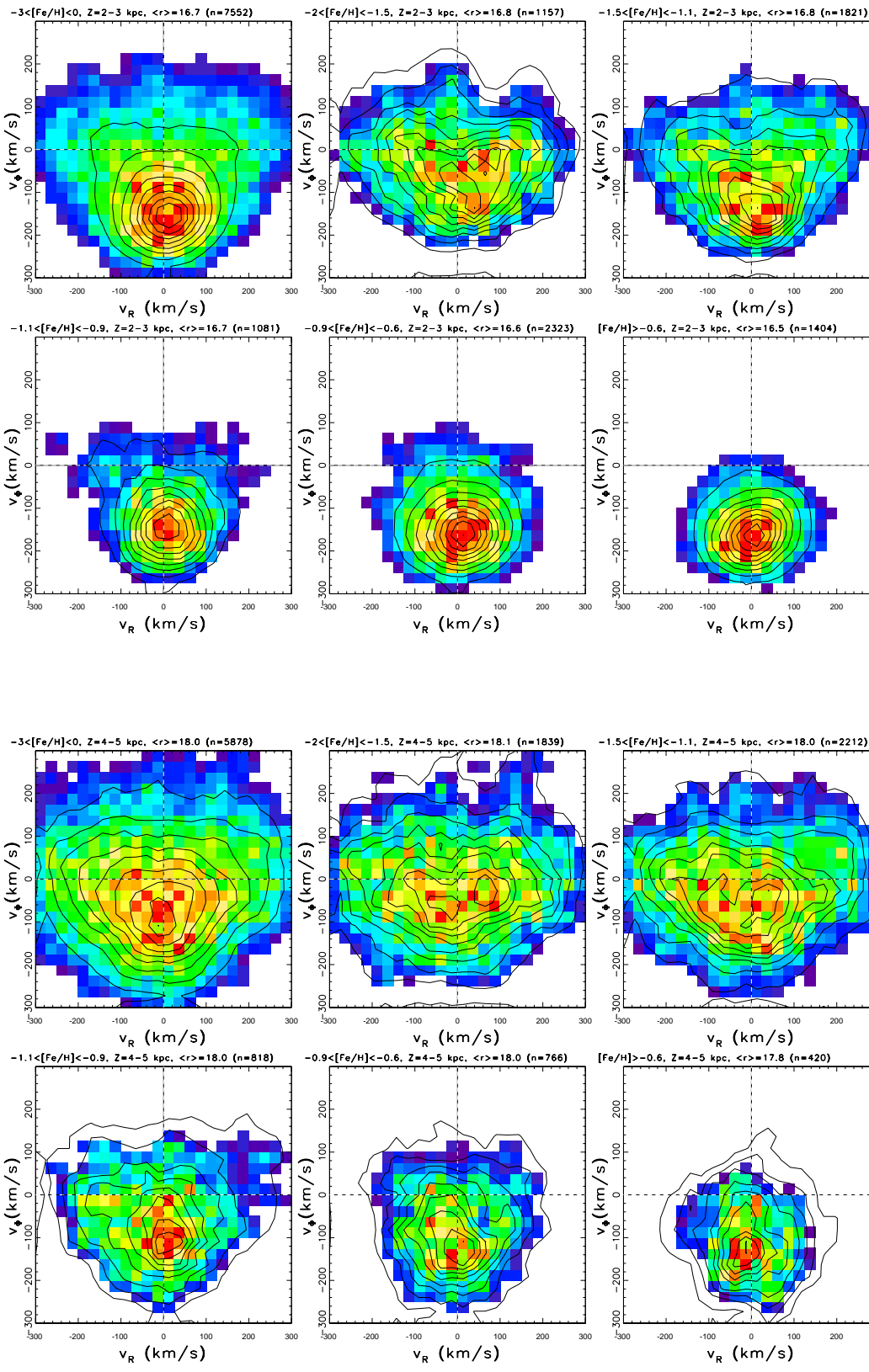
and so

$$\kappa_\odot = 36 \pm 10 \text{ km/s/kpc}, \quad (34)$$

and

$$\frac{\kappa_\odot}{\Omega_\odot} = 1.3 \pm 0.2 \quad (> 1 \text{ and } < 2!) \quad (35)$$

For improvements to epicycle approximation see Dehnen 1999
(AJ 118, 1190)

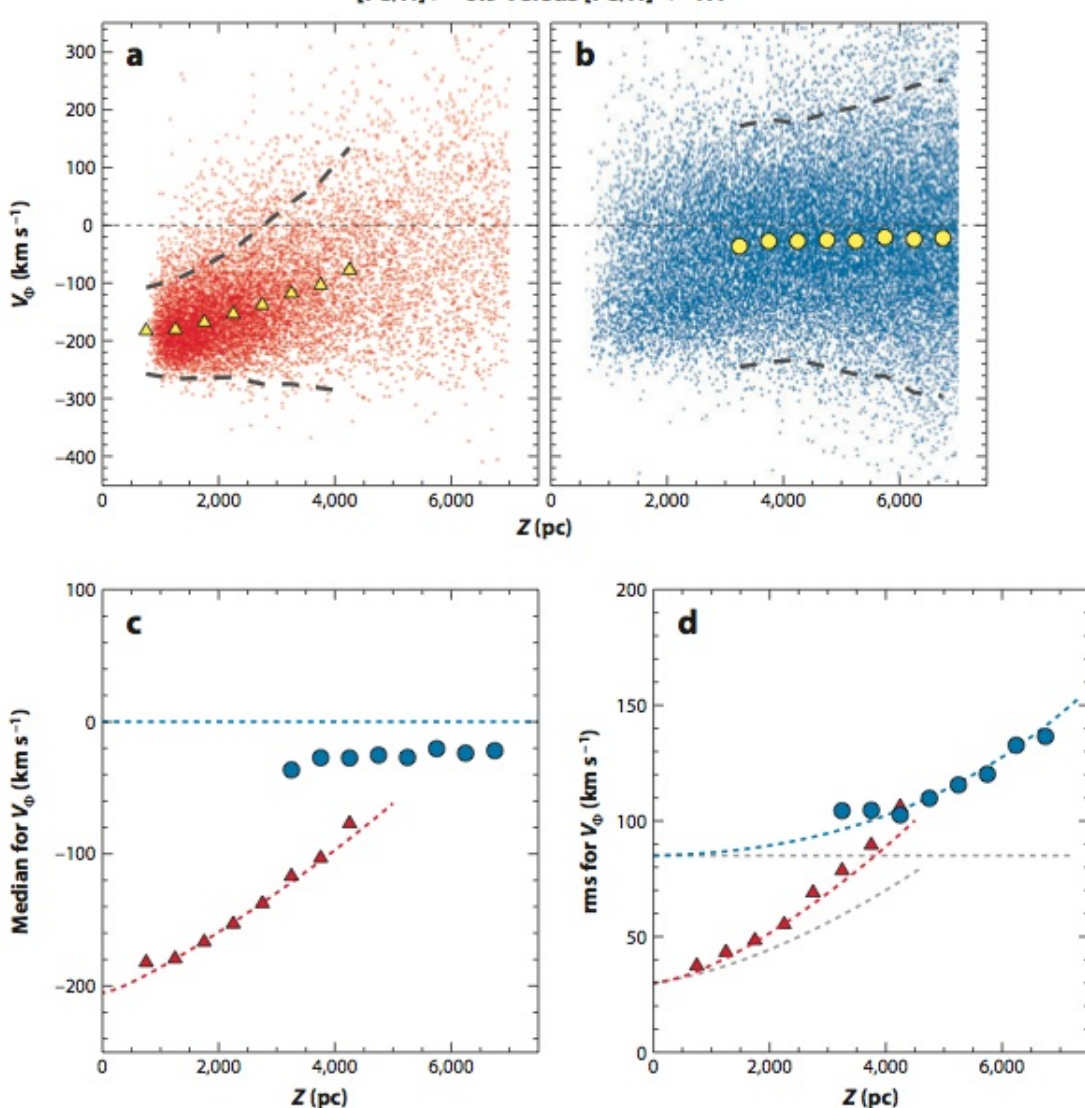


Kinematics for distant stars

- **Top panels:** $f(v_R, v_\phi)$ for blue (F and G) main-sequence stars towards the north galactic pole; determined using SDSS-POSS proper motions, $Z = 2 - 3$ kpc. The top left is the full sample, the other five are for $[Fe/H]$ slices, from -2 to > -0.6 (halo, halo, mixed, disk, disk)
- **Bottom panels:** analogous, for $Z = 4 - 5$ kpc.
- **Conclusion:** High-metallicity stars have net rotation (the median velocity depends on Z), low-metallicity stars are consistent with no rotation.

Disk vs. Halo Kinematics

- **Top panels:** small dots are individual stars, large symbols are the median values.
- **Top left:** disk stars show clear velocity shear (increase of v_ϕ with Z)
- **Top right:** halo stars $< v_\phi > \sim 220$ km/s
- **Bottom left:** velocity shear is **not** linear
- **Bottom right:** velocity dispersion slowly increases with Z for disk stars, while for halo stars it is spatially invariant



Is velocity shear simply a consequence of thick disk becoming dominant over thin disk beyond 1-2 kpc?

Is velocity shear simply a consequence of thick disk becoming dominant over thin disk beyond 1-2 kpc?

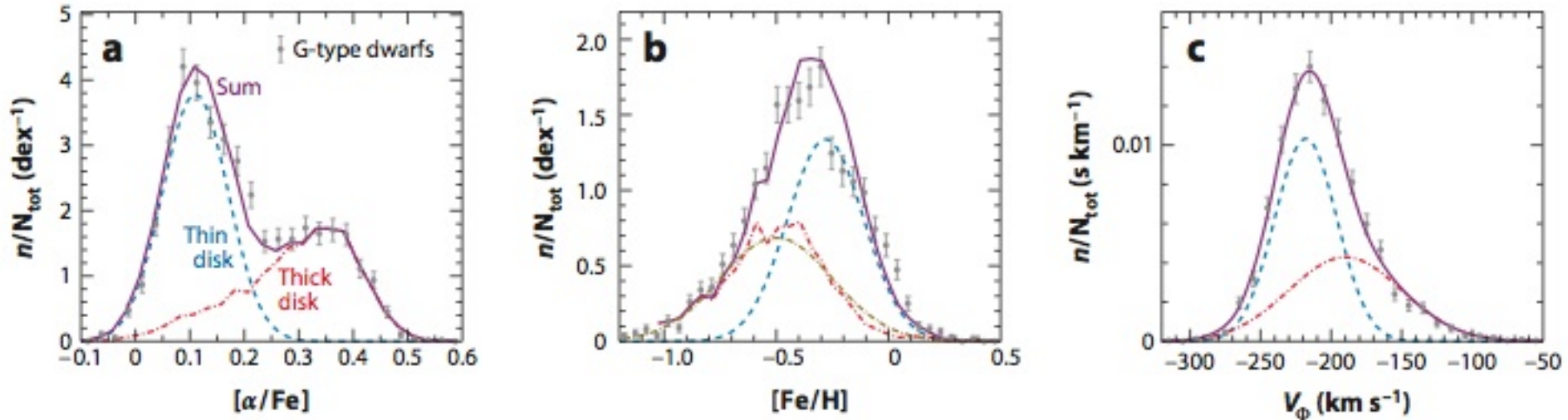
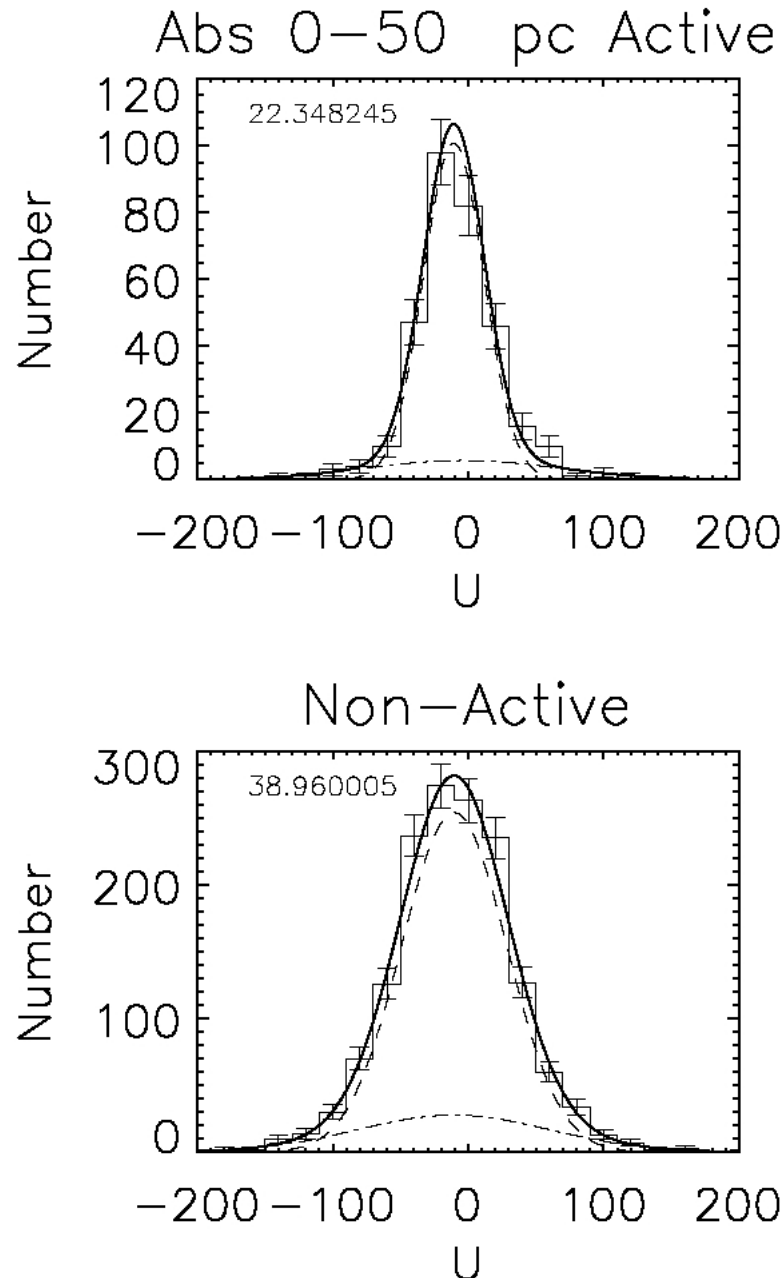


Figure 12

Tests of thin-/thick-disk decomposition using the sample of G-type dwarfs from Lee et al. (2011b). (a) The $[\alpha/\text{Fe}]$ distribution for $\sim 2,300$ stars in the fiducial bin $|Z| = 400\text{--}600$ pc as gray circle symbols with (Poissonian) error bars. The bimodality is easily seen. The observed distribution can be modeled as the sum (shown by the *purple solid line*) of two components: the $[\alpha/\text{Fe}]$ distribution for $\sim 3,300$ stars with $|Z| = 2\text{--}3$ kpc shifted to lower values by 0.03 dex (*red dot-dashed line*) and a Gaussian distribution, $N(0.11, 0.06)$ (*blue dashed line*). The weights for the two components (0.43 and 0.57 for the thick and thin components, respectively) are consistent with a double-exponential fit to star counts. (b) The $[\text{Fe}/\text{H}]$ distribution for the same stars from the fiducial $Z = 400\text{--}600$ pc bin as symbols with error bars. Similar to the $[\alpha/\text{Fe}]$ distribution, it can be modeled as the sum (purple solid line) of two components: the $[\text{Fe}/\text{H}]$ distribution for stars with $|Z| = 2\text{--}3$ kpc shifted to higher values by 0.2 dex (*jagged red dot-dashed line*) and $N(-0.28, 0.17)$ (*blue dashed line*). The weights for the two components (0.43 and 0.57) are the same as in panel a. The $[\text{Fe}/\text{H}]$ distribution for stars with $|Z| = 2\text{--}3$ kpc is well described by $N(-0.50, 0.25)$ (after application of a 0.2 dex offset), shown as the smooth dark yellow dot-dashed line. (c) The rotational velocity distribution for the same stars from the fiducial $|Z| = 400\text{--}600$ pc bin as symbols with error bars. It can be modeled as a linear combination of two Gaussian distributions, $N(-218, 22)$ and $N(-190, 40)$, again using the same relative weights (and line styles) as in panel a.

Scattering of Disk Stars



Bochanski et al.
(2007, AJ 134, 2418)

- Hot blue stars have smaller velocity dispersions than cool red stars; metal-rich stars have smaller velocity dispersions than metal-poor stars
- Active (presumably young) M dwarfs have smaller velocity dispersion than non-active M dwarfs (Bochanski et al. 2007)
- The imperfections in the Galaxy's gravitational field cause the random velocities of stars to increase: **the velocity dispersion increases with age: $\sigma \propto t^{1/2}$**
- The irregularities responsible for this phenomenon range in scale from small such as **molecular clouds**, to large such as **spiral arms**
- Can we (at least qualitatively) understand this behavior?

Scattering by molecular clouds

Typical clouds: up to $10^6 M_\odot$, < 100 pc

Spitzer & Schwarzschild (1953) proposed their existence, motivated by the correlation between the velocity dispersion and age, *before* the first ones were detected!

A star has a relative speed with respect to a cloud because of differential rotation. The successive encounters will increase the star's random velocity.

Prediction: $\sigma \propto t^{1/4}$ slower than observed

Another difficulty: can explain σ of up to 30 km/s, but white dwarfs and C stars have $\sigma \sim 50$ km/s

Scattering by spiral arms

N-body simulations: spiral arms can heat the disk

The spiral structure heats the disk, which decreases the efficiency of the swing amplifier until the spiral structure cannot be maintained.

“Thus the spiral structure is killed by the heat that it injects into the disk, just as yeast in a vat of fermenting beer is killed by the alcohol it creates” (from Binney & Tremaine).

Important: a fixed spiral pattern cannot heat the disk – the arms must be transitory (see BT figs. 7-26 and 7-27)

Note that within Lin-Shu theory disk heating is negligible; the stochastic theory predicts significant disk heating

Prediction: $\sigma \propto t^\alpha$, with $\alpha \sim 0.2 - 0.5$ not too bad

Scattering by spiral arms

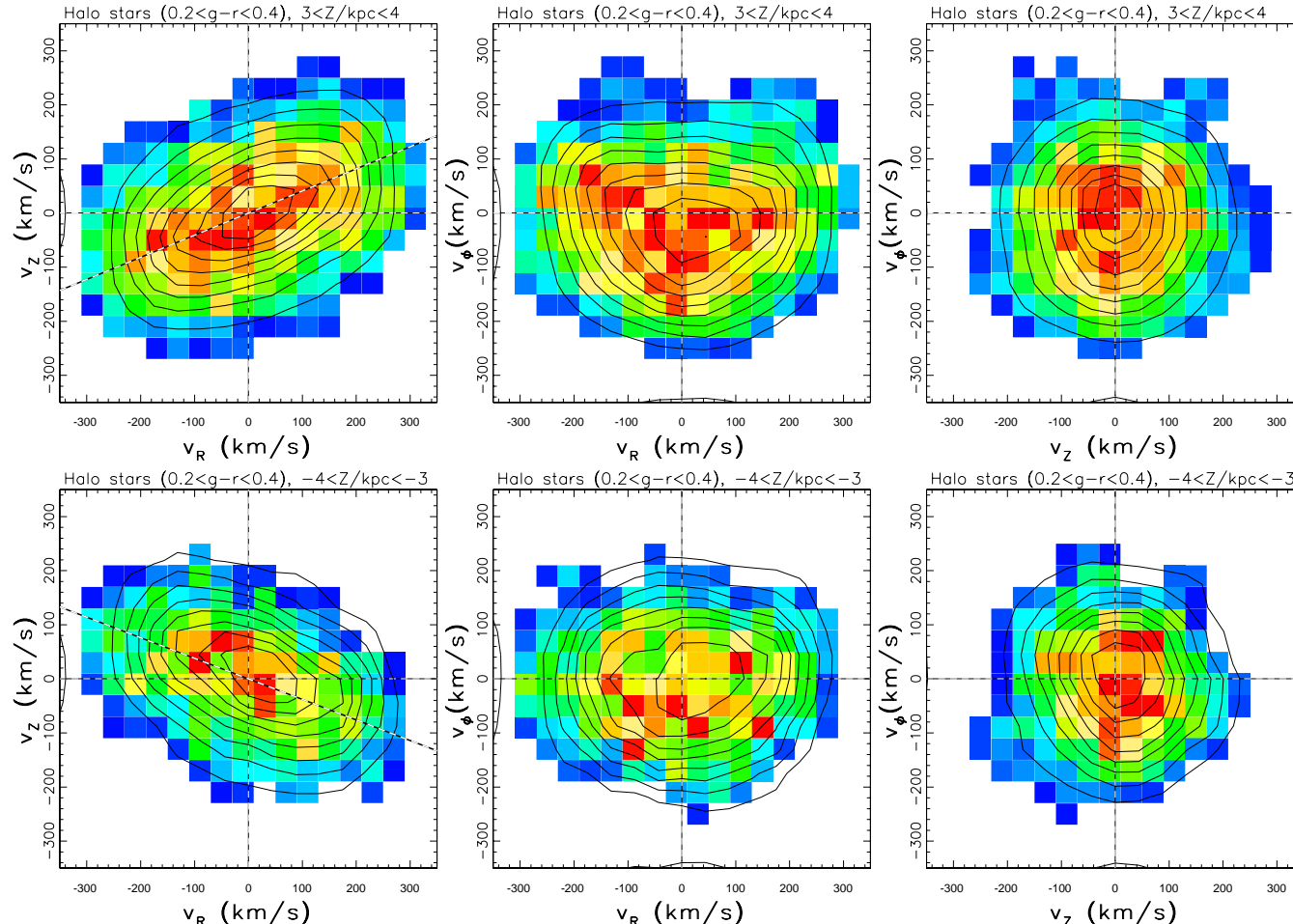
Problem: the velocity dispersion increases only in the radial and azimuthal directions. What about the vertical dispersion?

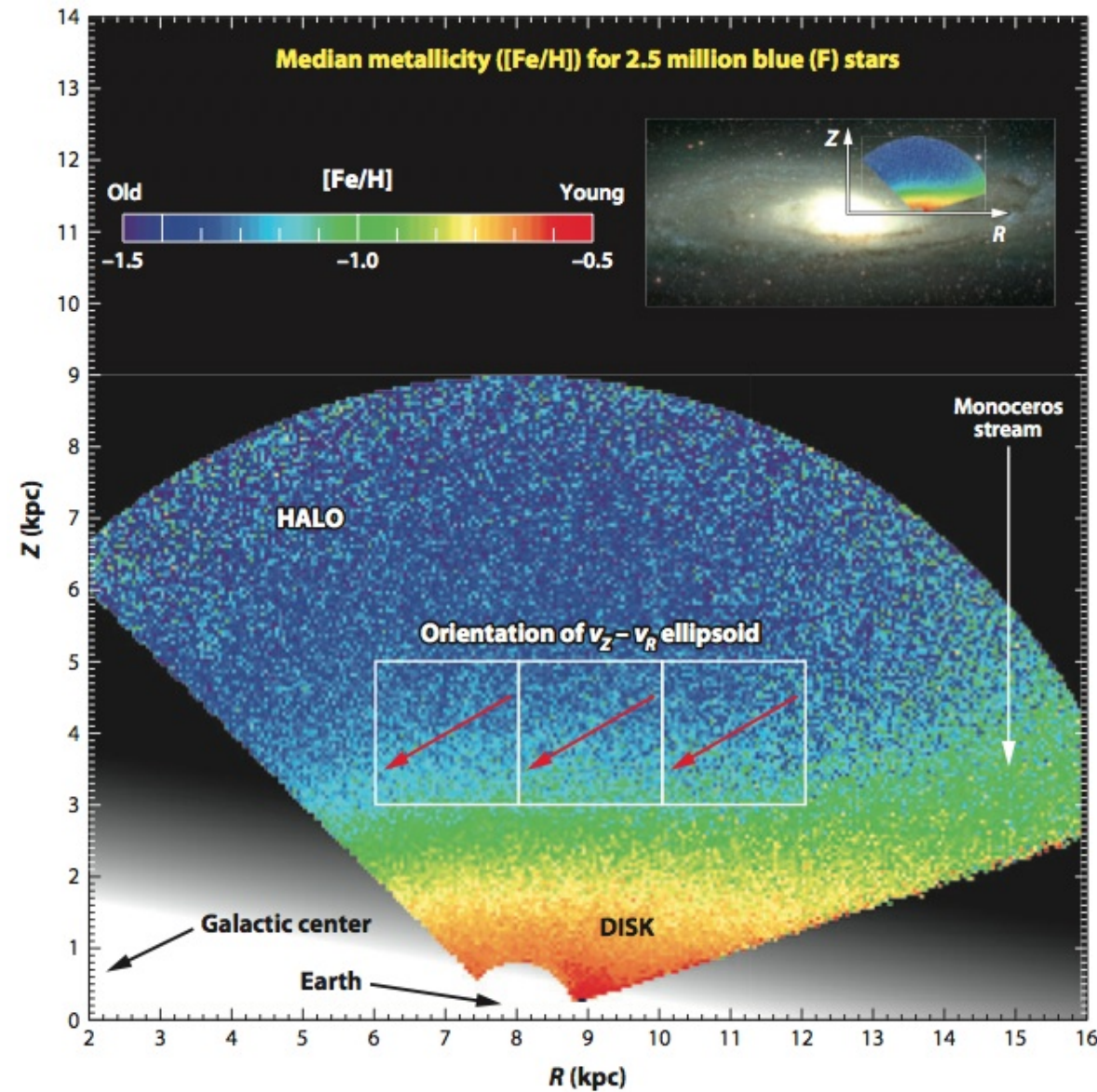
Carlberg (1984): spiral arms provide heating in the radial and azimuthal directions, which molecular clouds redistribute in the vertical direction.

Lacey & Ostriker (1985): the heating is due to $10^6 M_\odot$ black holes from the halo.

Halo Velocity Ellipsoid Tilt

- Three two-dimensional projections of the velocity distribution for two subsamples of candidate halo stars ($[Fe/H] < -1.1$) with $6 < R/\text{kpc} < 11$, and $3 < Z/\text{kpc} < 4$ (top) and $-4 < Z/\text{kpc} < -3$ (bottom)
- The v_Z vs. v_R velocity ellipsoid is aligned with spherical coordinate system (Bond et al. 2010). Confirms results of Smith et al. (2009) over 30 times larger area.





A comparison of counts,
metallicity distribution and
kinematics.

- The arrows illustrate the variation of the ellipsoid orientation, which **always points toward the Galactic center!**
- This measurement can be used to infer the shape of gravitational potential (Loebman et al. 2012, ApJ 758, L23, see later).

The Local Mass Density

The v_z Jeans equation (steady-state):

$$\frac{\partial(\nu \bar{v}_R v_z)}{\partial R} + \frac{\partial(\nu \bar{v}_z^2)}{\partial z} + \frac{\nu \bar{v}_R v_z}{R} + \nu \frac{\partial \Phi}{\partial z} = 0.$$

Drop the first and third terms because they are a factor of $\approx z^2/(RR_d)$ smaller than the second and fourth terms:

$$\frac{1}{\nu} \frac{\partial(\nu \bar{v}_z^2)}{\partial z} = - \frac{\partial \Phi}{\partial z} \quad (36)$$

Near the plane of a highly flattened system, Poisson's equation becomes

$$\frac{\partial^2 \Phi}{\partial z^2} = 4\pi G \rho \quad (37)$$

The Local Mass Density

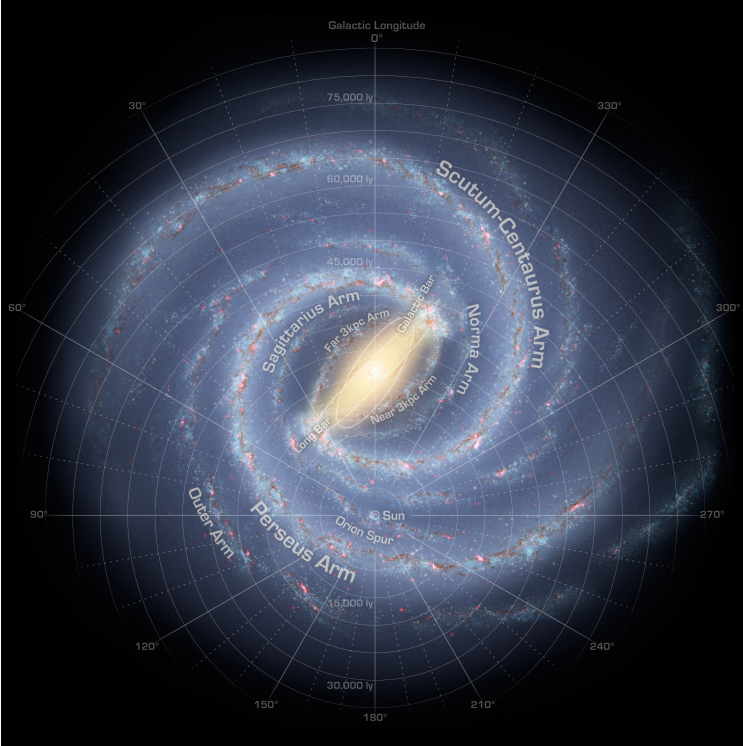
$$\frac{\partial}{\partial z} \left[\frac{1}{\nu} \frac{\partial(\nu \bar{v}_z^2)}{\partial z} \right] = -4\pi G \rho \quad (38)$$

If we can measure ν and \bar{v}_z^2 (as functions of z), then we can determine the local mass density ρ , which also includes *dark matter* component, if any. This ρ is called the Oort limit.

Oort (1932) estimated $\rho(R_\odot, z = 0) = 0.15 \text{ M}_\odot/\text{pc}^3$.

Bahcall (1984) estimated $\rho(R_\odot, z = 0) = 0.18 \pm 0.03 \text{ M}_\odot/\text{pc}^3$. This appeared as a significant result because the local density of the luminous matter (stars, gas and white dwarfs) is estimated at $0.11 \text{ M}_\odot/\text{pc}^3$, and thus suggests the existence of dark matter in the disk (the halo dark matter contribution to local ρ is less than $0.01 \text{ M}_\odot/\text{pc}^3$).

However, Kuijken & Gilmore (1989, MNRAS 239, 651) showed that previous samples and analysis were flawed: there is no evidence that the dynamical mass density is larger than the local density of the luminous matter – both are around $0.10 \text{ M}_\odot/\text{pc}^3$.

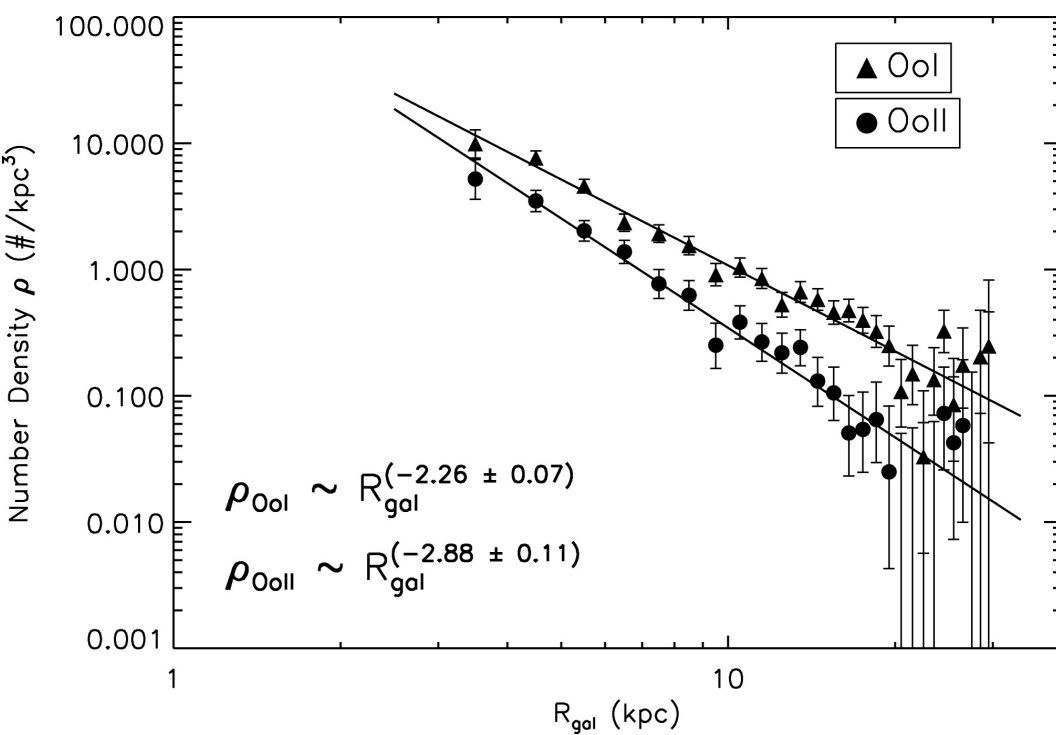
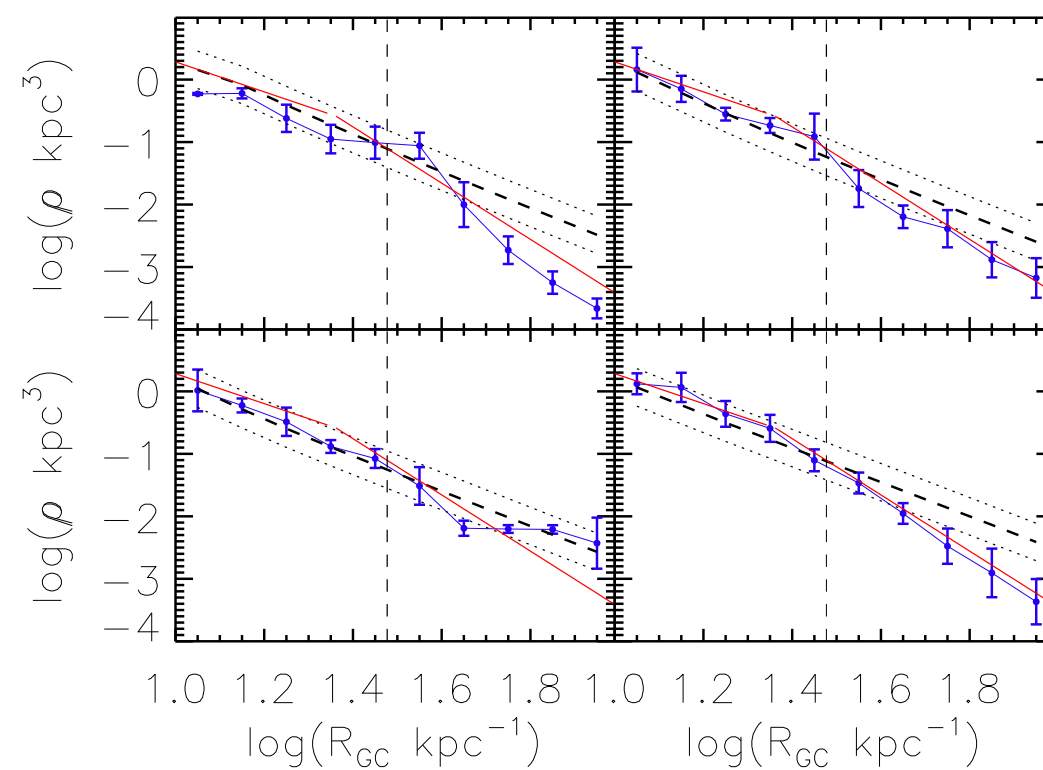


Outer halo studies: RR Lyrae from SDSS Stripe 82

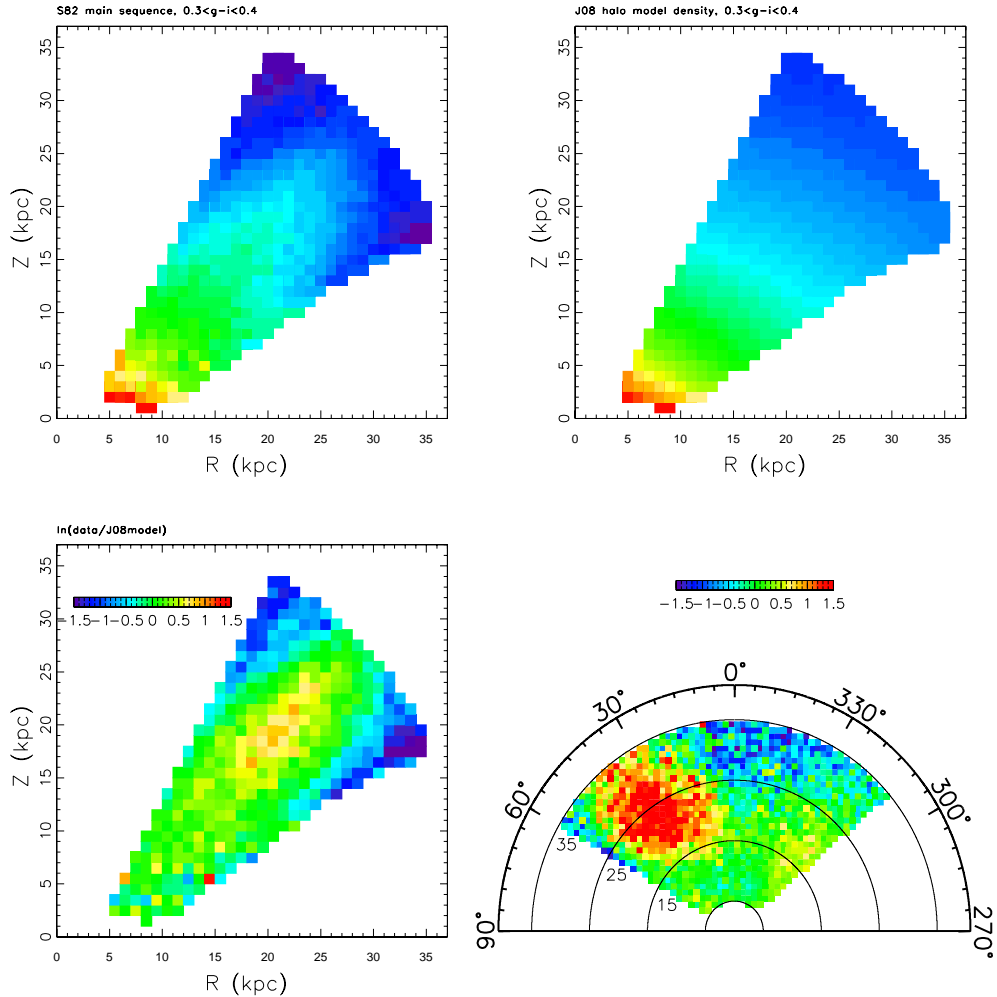
- **Top left:** the disk structure (artist's conception based on the Spitzer and other surveys of the Galactic plane)
- **Bottom left:** the halo density (multiplied by R^3 ; yellow and red are overdensities relative to mean $\rho(R) \propto R^{-3}$ density) as traced by ~ 500 RR Lyrae from SDSS Stripe 82 (Watkins et al; Sesar et al. 2009), compared in scale to the top panel
- **Conclusions:** the spatial distribution of halo stars is highly inhomogeneous (clumpy); when averaged, the stellar volume density decreases as $\rho(R) \propto R^{-3}$.

Outer halo studies: RR Lyrae from SDSS Stripe 82

- **Top left panels:** four regions selected by R.A.; points: observed density, blue line: fit from Sesar et al. (2009); red lines: fit from Watkins et al. (2009); similar results for 2016 candidate RR Lyrae from SEKBO survey (Keller et al. 2008);
- **Bottom left panel:** Oosterhof I and II profiles for 838 LO-NEOS RR Lyrae from Miceli et al (2008); confirmed by stripe 82 RR Lyrae
- **Conclusions:** The density profile steepens beyond ~ 30 kpc; within 30 kpc, the profile for Oosterhof II subset is steeper



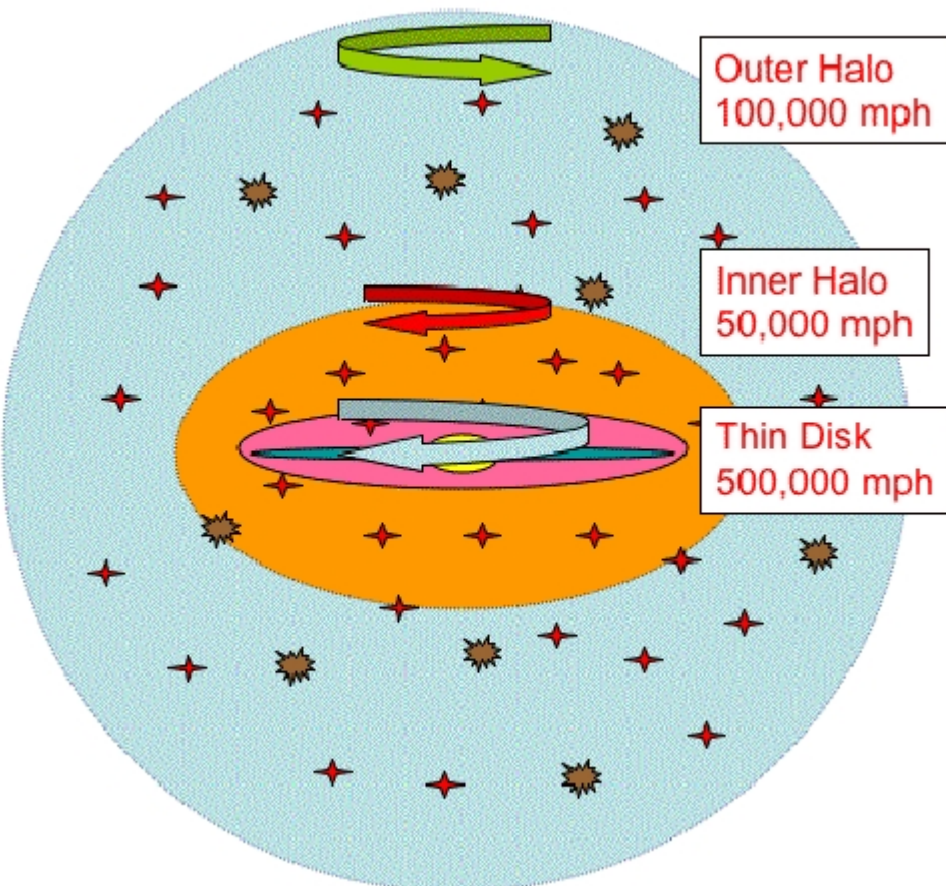
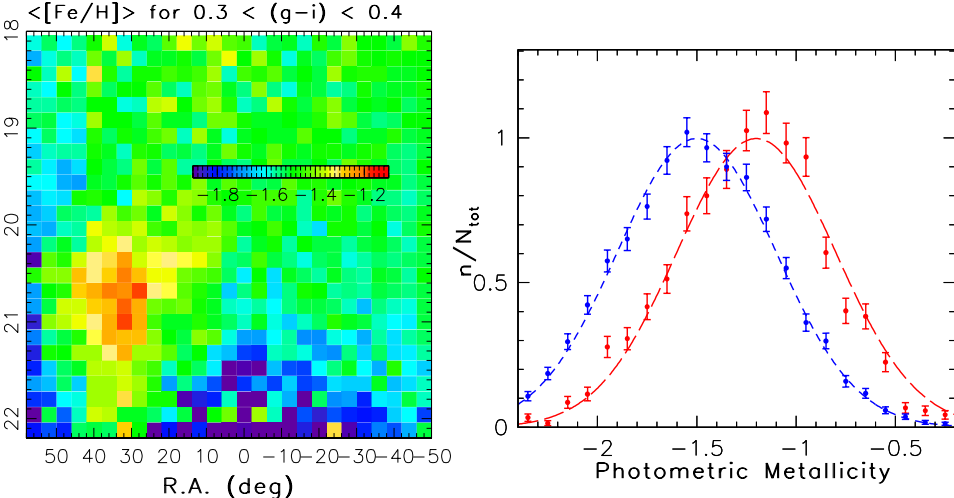
Outer halo studies: main-sequence stars



- Sesar et al. (2009): co-added SDSS Stripe 82 data enable mapping with numerous main-sequence stars out to ~ 30 kpc
- **Top left:** Observed density map
- **Top right:** Galfast model prediction
- **Bottom left:** Data/model ratio, overdensity is the Sgr tidal stream
- **Bottom right:** Data/model ratio along the celestial equator
- Evidence for steepening of the density profile beyond ~ 20 kpc from the Galactic center
- Consistent conclusion with the RR Lyrae spatial profile

Outer halo studies: main-sequence stars

- Evidence for steepening of the density profile beyond ~ 20 kpc from the Galactic center
- Top left: evidence for drop in metallicity of smooth background halo beyond $\sim 20\text{-}30$ kpc
- However, high surface-brightness overdensities have higher $[Fe/H]$, top right Supports simulation-based results by, e.g., Johnston et al. (2008) and Zolotov et al. (2009)
- Agrees with indirect results based on kinematics from Carollo et al. (2007) and Carollo et al. (2010), bottom panel



Tentative Summary of Direct Halo Measurements

1. $\rho(R, Z, \phi)$:

- Within ~ 10 kpc traced by main-sequence stars; oblate ($q = 0.64 \pm 0.1$), $\rho \sim 1/R^3$ ($n = 2.8 \pm 0.2$)
- Within ~ 100 kpc traced by RR Lyrae stars; a steeper slope beyond 30 kpc and much more substructure, extends to at least ~ 100 kpc, within 30 kpc Oosterhof II subset have a steeper slope

2. $[Fe/H]$:

- Within ~ 10 kpc traced by main-sequence stars; uniform gaussian distribution (gradient < 0.01 dex/kpc) centered on $[Fe/H] = -1.5$ with a dispersion of 0.3 dex

- Beyond \sim 20-30 kpc, $[Fe/H]$ for the background diffuse population probably decreases; however, for high surface brightness substructure $[Fe/H] > -1.5$ (Sgr trailing tidal tail: $[Fe/H] = -1.2$, Monoceros stream: $[Fe/H] = -1.0$)

3. **Kinematics:**

- Within \sim 10 kpc traced by main-sequence stars, no rotation to within 10-20 km/s, velocity ellipsoid aligned with the spherical coordinate system: $\sigma_R = 140$ km/s, $\sigma_\phi = 85$ km/s, $\sigma_\theta = 75$ km/s
- Limited data beyond 10 kpc; based on a heterogeneous sample of \sim 250 objects, it appears that beyond \sim 30 kpc the radial velocity dispersion is decreasing with R (to \sim 50 km/s at \sim 120 kpc).

Indirect measurements by Carollo et al. in qualitative agreement.

(Dark) Halo mass density profile

The Jeans equation for a steady-state rotationally invariant spherical system (see notes from Tom's class and extra lecture on kinematics theory):

$$\frac{1}{\nu} \frac{d(\nu \sigma_r^2)}{dr} + \frac{2\beta \sigma_r^2}{r} = -\frac{d\Phi}{dr}$$

where $\beta = 1 - (\sigma_\theta/\sigma_r)^2$ (note that here “r” is the spherical galactocentric radius).

With $d\Phi/dr = GM(r)/r^2$, we can translate SDSS results to a constraint on $M(r)$. For example,

- Jurić et al. (2008) obtained for halo: $\nu(r) \propto r^{-2.8}$
- Bond et al. (2010) list $\sigma_r = 141$ km/s, $\sigma_\theta = 75$ km/s, and $\sigma_\phi = 85$ km/s

(Dark) Halo mass density profile: spherical case

Ignoring for a moment that Jurić et al. (2008) obtained an oblate halo ($c/a = 0.64$), and that σ_θ and σ_ϕ are not equal (assume $\beta = 0.68$), it is easy to show that $M(r) \propto r$.

This $M(r)$ behavior implies a logarithmic gravitation potential $\Phi(r) = v_c^2 \ln(r/r_c)$, where v_c is the circular velocity, and r_c is a characteristic spatial scale.

More importantly, we also get $\rho(r) \propto r^{-2}$, where $\rho(r)$ includes **all** the matter!

This profile is the so-called “iso-thermal” profile and implies a flat rotation curve.

But what about the fact that we ignored departures from spherical symmetry for the halo density law?

(Dark) Halo mass density profile: non-spherical case

Smith et al. (2009) give relevant references and nicely summarize a generalization to an axially symmetric case (based on logarithmic potential): for **stellar** density given by

$$\nu(r, \theta) = \nu_0 r^{-\gamma} [\sin(\theta)]^{2n} \quad (39)$$

one expects the following relations between the velocity dispersions:

$$\sigma_r = \text{const.} \quad (40)$$

$$(\sigma_\theta/\sigma_r)^2 = \frac{m + n + 1}{n + 1}, \quad (41)$$

and

$$(\sigma_\phi/\sigma_\theta)^2 = 2n + 1, \quad (42)$$

where m , n and γ can be constrained by velocity dispersion data.

(Dark) Halo mass density profile: non-spherical case

Smith et al. model $\nu(r, \theta)$ as a linear combination of the two lowest terms with $n = 0$ and $n = 1$,

$$\nu(r, \theta) = \nu_0 r^{-\gamma} (1 + \nu_1 [\sin(\theta)]^2) \quad (43)$$

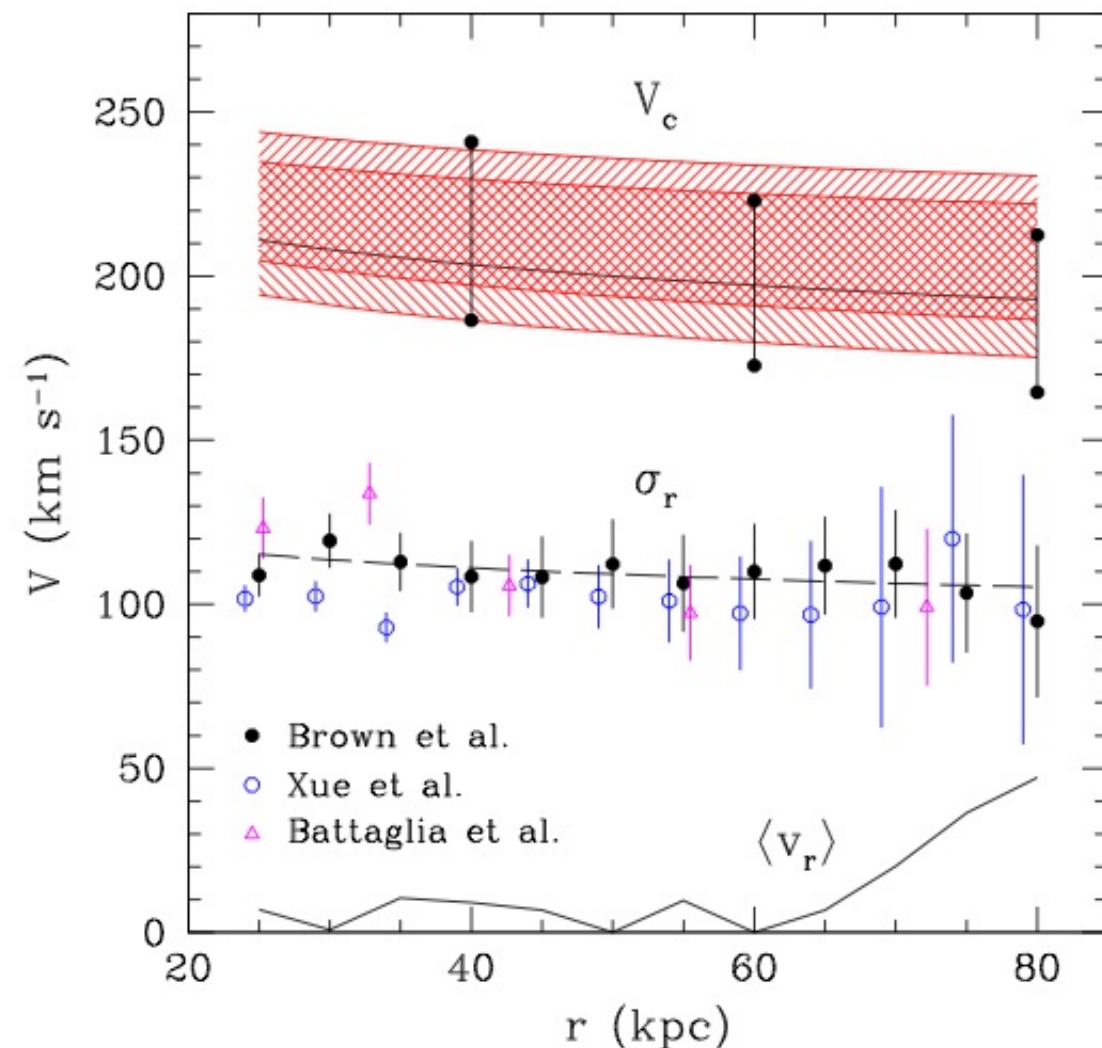
and obtain $(\nu_1/\nu_0)=0.063$ ($q = 0.983$), $m = -0.72$ and $\gamma = 3.75$ (their velocity dispersions, based on main sequence stars, are not measured as functions of positions, so they assumed that they are constant).

However, since their measured σ_ϕ and σ_θ (from SDSS Stripe 82) are consistent within error bars, their result for (ν_1/ν_0) must be consistent with 0 (though they don't say it).

Does the radial velocity dispersion vary in the outer halo?

Halo radial velocity dispersion: profile at large radii

- Does the radial velocity dispersion vary in the outer halo?
- Data show only a little bit of gradient between ~ 10 kpc and ~ 100 kpc: Gnedin et al. (2010) get a power-law index of -0.08 .
- If recent SDSS-based values from Bond et al. (2010) and Smith et al. (2009) are added, then the power-law index becomes -0.12 .
- **We need better kinematic data in the 10-100 kpc distance range.**



Gnedin et al. (2010, ApJ 720, L108)

A smooth global kinematic model is possible...

- Overall kinematic behavior can be captured by a simple model

18

BOND ET AL.

Vol. 716

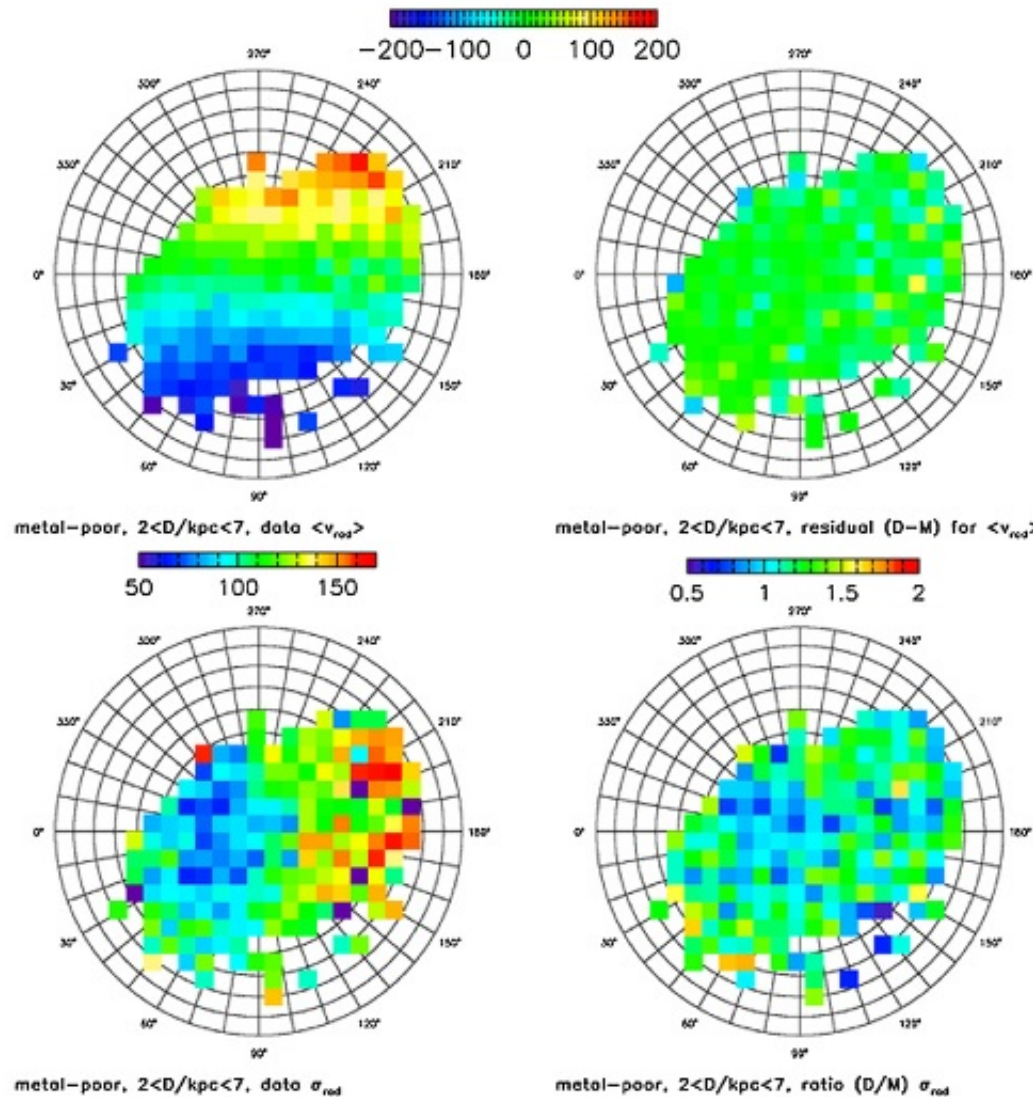


Figure 16. Comparison of medians and dispersions for the measured and modeled radial velocities of 20,000 blue ($0.2 < g - r < 0.4$) halo stars (spectroscopic $[\text{Fe}/\text{H}] < -1.1$) at distances, $D = 2 - 7$ kpc, and $b > 20^\circ$. The top-left panel shows the median measured radial velocity in each pixel, color-coded according to the legend shown at the top (units are km s^{-1}). The top-right panel shows the difference between this map and an analogous map based on model-generated values of radial velocity, using the same scale as in the top-left panel. The bottom-left panel shows the dispersion of measured radial velocities, color-coded according to the legend above it. The bottom-right panel shows the ratio of this map and an analogous map based on model-generated values of radial velocity, color-coded according to the legend above it. When the sample is divided into 1 kpc distance shells, the behavior is similar.

A smooth global kinematic model is possible...

- for both low- and high-metallicity components

22

BOND ET AL.

Vol. 716

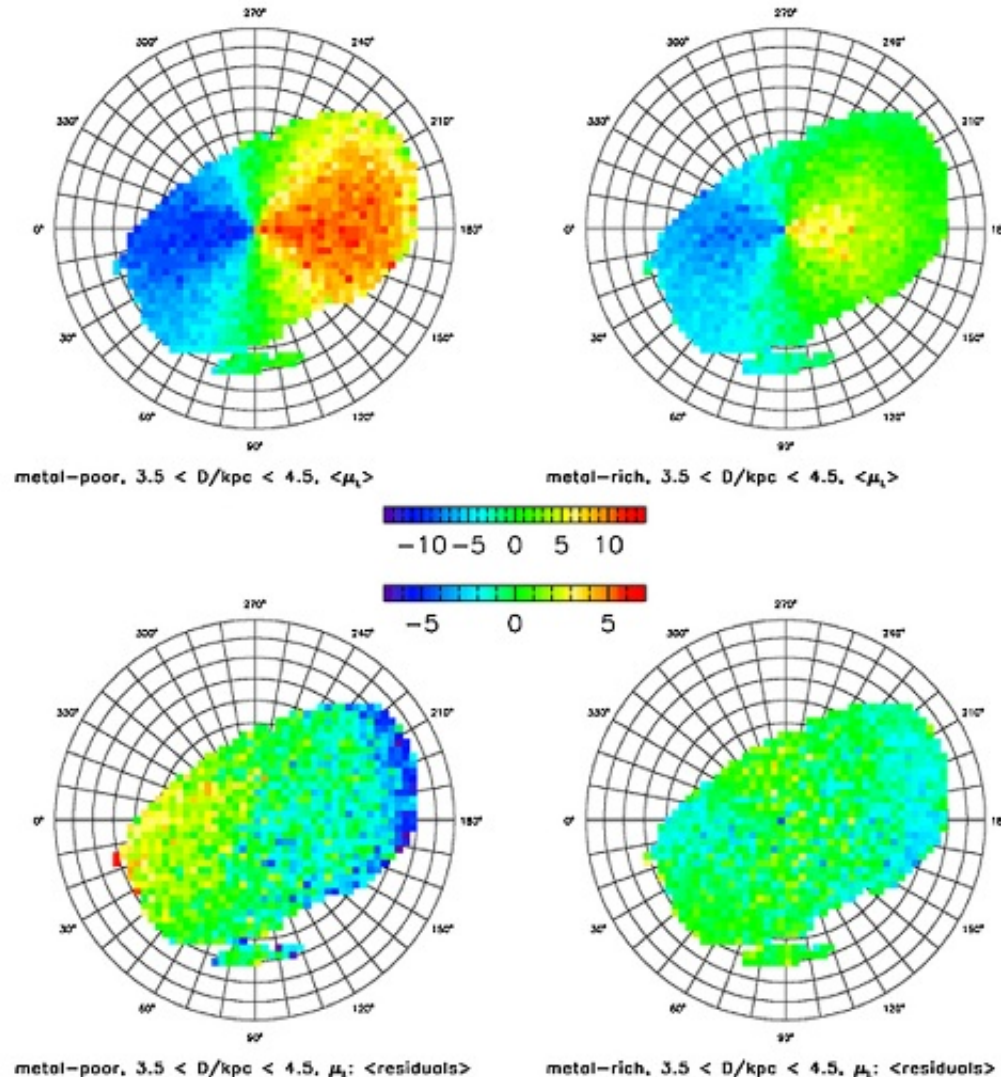


Figure 20. Similar to Figures 17 and 19, except that the behavior of high-metallicity (left) and low-metallicity (right) stars is compared in a single distance bin (3.5–4.5 kpc). The top two panels show the median longitudinal proper motion, and the two bottom panels show the median difference between the observed and model-predicted values. An analogous figure for the latitudinal proper motion has similar characteristics.

Empirical Model for Mock Catalogs: **Galfast**

- Web service by Mario Jurić based on smooth spatial, metallicity and kinematics distributions measured by SDSS
- Available from www.mwscience.net/galfast
- A valuable tool when searching for substructure in data, or comparing to theoretical models
- For example, can easily make mock catalogs for surveys such as SDSS, SkyMapper, Pan-STARRS, Gaia, and LSST

File Edit View History Bookmarks Tools Help

http://hybrid.mwscience.net/galfast/?jobid=4

mwscience.net :: Galactic Model Generator BETA :: Mario Juric :: Mon Aug 3 05:21:28 2009

New mock catalog Catalog list Logout Help

Job Options

Description: Flux limited/volume cut LSST sample

E-mail for notification: majuric@gmail.com

Send e-mail on completion:

Random seed: 42

Output in FITS format:

Skip Q/A plot generation:

Make this a template for new jobs:

Model

Maximum stars to generate: 50e6

Density Components:

Exp Disk and Power Law Halo (model_5cc3d9.conf):

Model type: Exp Disk and Power Law Halo

Enabled:

Solar offset (Z_\odot): 24

Thin disk parameters ($\rho_0, L1, H1$): 1, 2150, 245

Thick disk parameters ($f_D, L2, H2$): 0.13, 3261, 743

Halo parameters (f_H, n_H, q): 0.0051, 2.77, 0.64

Cutoff radius (r_{cut} in pc): 100000

Luminosity function band (M_{-X}): LSSTZ

Luminosity function, $\Phi(M_{-X})$: MzLF.lf.txt

Observed area:

Pencil Beam (foot.196ea.conf):

Save changes Queue Clone Remove Clean Delete

Done

Double-exponential density profile (with Jurić et al. 2008, defaults)

This model describes the density in terms of three components: the thin and thick disks (double-exponentials), and a power-law halo. The profiles are as follows:

$\rho(R, Z) = \rho_{thin}(R, Z) + \rho_{thick}(R, Z) + \rho_H(R, Z)$

$\rho_{thin}(R, Z) = \rho_0 e^{\frac{R_\odot}{L_1}} \exp\left(-\frac{R - Z + Z_\odot}{H_1}\right)$

$\rho_{thick}(R, Z) = f_D \rho_0 e^{\frac{R_\odot}{L_2}} \exp\left(-\frac{R - Z + Z_\odot}{H_2}\right)$

$\rho_H(R, Z) = \rho_0 f_H \left(\frac{R_\odot}{\sqrt{R^2 + (Z/q_H)^2}}\right)^{n_H}$

Mock catalog: sky.fits (0.1 MB)

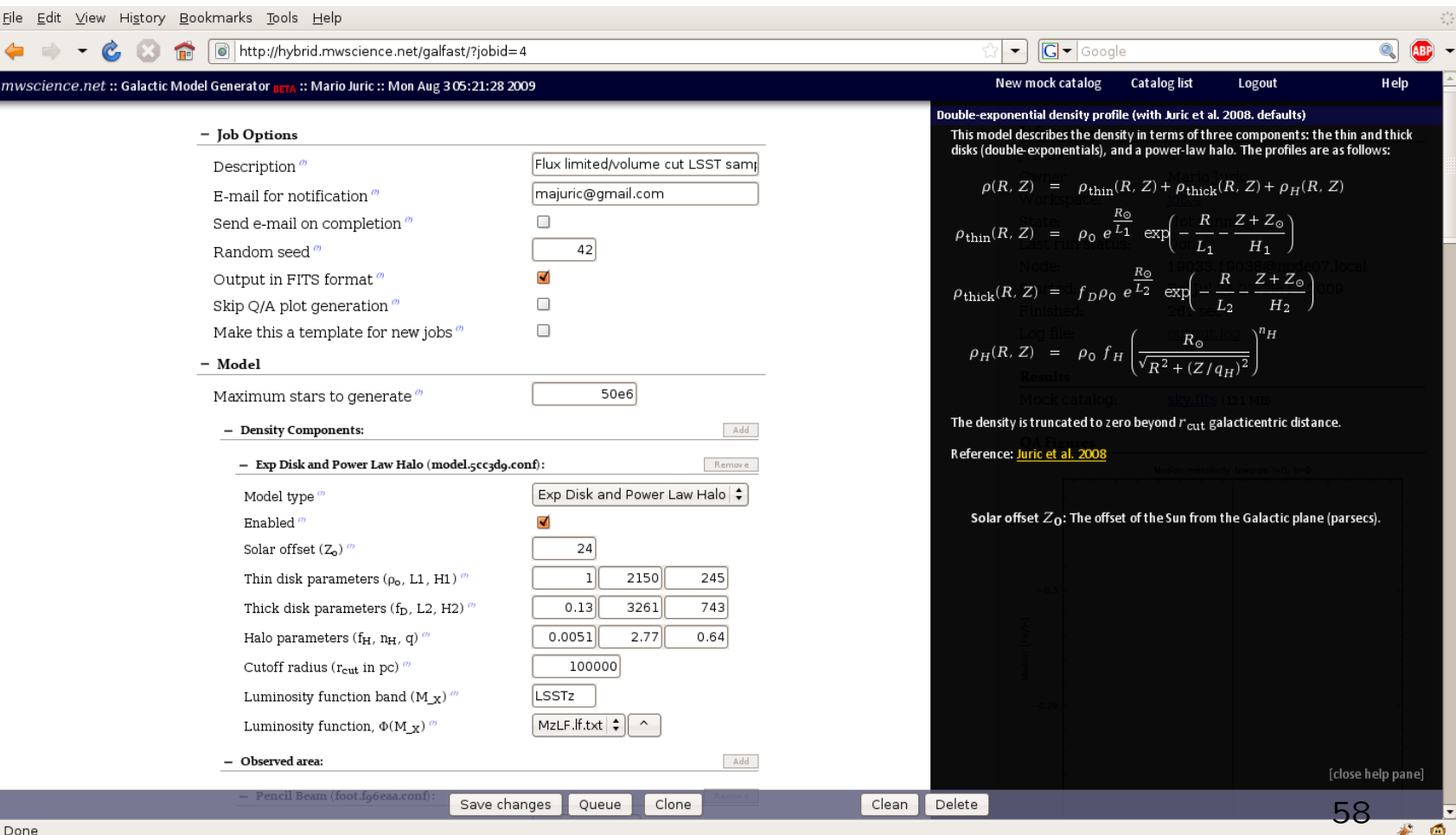
The density is truncated to zero beyond r_{cut} galactocentric distance.

Reference: [Jurić et al. 2008](#)

Solar offset Z_\odot : The offset of the Sun from the Galactic plane (parsecs).

Median metallicity towards $l=0, b=0$

[close help pane]



Summary of Metallicity/Kinematics Results

- Clumps/overdensitiesstreams are an integral part of Milky Way structure, both for halo and disk components; the kinematics and metallicity distribution are exceedingly complex.
- Nevertheless, it is possible to construct a reasonably good model for the smooth global behavior (Bond et al. 2010)
- The rotational lag (velocity shear) and metallicity distribution for disk stars are **smooth** functions of Z
- The halo velocity ellipsoid is invariant in spherical coordinates (within 10 kpc or so).

SDSS has revolutionized studies of the Galactic structure;

Gaia and LSST will do even better! (the last lecture)